Nonlinear Approaches to Predicting Diameter of the Largest Limb at Breast Height in Young, Douglas-fir (Pseudotsuga menziesii (Mirbel) Franco) Plantations Growing in the Pacific Northwest

Jedediah Syc Bryce

A thesis submitted in fulfillment of the requirements for the degree of

Master's of Science

University of Washington

2012

Reading Committee:

Eric Turnblom, Chair

Jim Flewelling

David Briggs

Program Authorized to Offer Degree:
School of Environmental and Forest Sciences

University of Washington

Abstract

Nonlinear Approaches to Predicting Diameter of the Largest Limb at Breast Height in Young, Douglas-fir (Pseudotsuga menziesii (Mirbel) Franco) Plantations Growing in the Pacific Northwest

Jedediah Syc Bryce

Chair of the Supervisory Committee:
Associate Professor Eric Turnblom
School of Environmental and Forest Sciences

This study examined two nonlinear modeling methodologies to predict the diameter of the largest limb at breast height ($DLLBH$) in young, Douglas-fir (*Pseudotsuga menziesii* (Mirbel) Franco) plantations in the Pacific Northwest using a combined power exponential function. The first method examined admitting predictor variables as additional factors in the power function portion and linear terms in the exponential portion. The second method used DBH as the base factor and estimated the parameters with simple linear functions of tree- and stand- variables. The second method proved superior as it simplified the model forms and preserved the allometric relationship between $DLLBH$ and DBH. $DLLBH$ was predicted with a residual standard error of .1627 and AIC of -13,398. Using $DLLBH$ as a surrogate for product recovery, the final model was used in the context of process capability analysis, where thresholds were set on $DLLBH$ and predicted cumulative distributions were generated in order to show how suppliers or purchasers might use the model in order check conformance of lumber to particular standards.

TABLE OF CONTENTS

LIST OF FIGURES

LIST OF TABLES

ACKNOWLEDGMENTS

In undertaking this particular project, I would like to extend my thanks to many people. First, to my committee members: Eric Turnblom, David Briggs, and Jim Flewelling for their invaluable advice and encouragement, even amidst committing novice mistakes. Without them I would have been unable to obtain this project and funding throughout my student life at the University of Washington. I attribute the majority of my knowledge to them, despite numerous informative classes.

I would also like to thank my officemate Kevin Ceder for extensive help in my LaTeX formatting endeavors, programming in R, and hospitality. To Bob Gonyea, Bert Hasselberg and everyone on the SMC field crew who have worked so hard the last $2\frac{1}{2}$ decades putting together such a great database. Without their fieldwork a database like this would not exist. To Megan O'Shea and all her help with funding and job searches. To Greg Ettl who provided the final funding to finish this project. Finally, to my family who have encouraged me throughout my master's degree.

Chapter 1
INTRODUCTION

1.1 Motivation

As branches grow and develop they become knots in wood, which are one of the primary structural features that diminish the quality of lumber and remanufactured wood products. This, coupled with the proportion of juvenile wood (based on the first 20 rings), ring width, and wood stiffness affect recovery, machine stress ratings and value of lumber [2], [9], [14]. For a log consisting of 25% juvenile wood, the recovery of quality grade Douglas-fir lumber drops 40% with an increase in knot size from .5 in. to 1.5 in. [10]. This, along with the fact that predicted lumber grade recovery is a continuous function of the largest limb average diameter ($LLAD$[1]) means small increases in branch diameter have detrimental consequences on recovery even though logs are graded in discrete sections. Though the amount of juvenile wood is important in determining the quality of lumber, it becomes less important as the knot sizes increase [7].

Recent decades have seen a decline in the quality of Douglas-fir lumber in the Pacific Northwest in part due to lower density planting that promotes greater stem development and consequently, greater branching and crown development [2], [7]. Understanding the effects of density management on the subsequent quality of wood is necessary for forest management given shorter rotation cycles and multiple uses of forest products. While people have studied the growth and development of branches coupled with the effects of initial spacing and thinning [1] in connection to wood quality, until recently there has been a lack of emphasis in the management of branches

[1]The average diameter of the largest limb in each log quadrant [10]

as they relate to knots [6].

This study aims to predict the diameter of the largest limb at breast height ($DLLBH$, 4.5 ft.) based on common tree- and stand-level metrics. It has been established that basic tree measurements suffice due to the allometric relationship between the size of the stem and its corresponding components [27], and while DBH may be the most important determinant of $DLLBH$, planting density is often of importance but to a lesser extent [24]. Emphasis is placed on the $DLLBH$ due to the lengthy time investment required to measure branches on the entire stem. Given that it is a quick, nondestructive measurement it can be incorporated in a timber cruise in order to gauge the potential quality of wood. In the past, other metrics have also been proposed, including $LLAD$ [10], number, volume, branch basal area, and wood area index (WAI[2]) [23]. While these are seen to be effective indications of product quality, the measurements are more cumbersome than $DLLBH$ and may not as easily be included with basic forest measurements. Furthermore, $DLLBH$ equations can be linked to $LLAD$ equations, which can then complete the product value chain [6], [8], [23]. During the past several decades both fixed- and mixed-effects models in linear and nonlinear forms have been used to describe abovementioned branch characteristics in multiple commercially relevant species, most notably: loblolly pine [1], lodgepole pine [2], black spruce [4], Douglas-fir [10], Scots pine [16], [17], [23], Corsican pine [18], Norway spruce [24] and radiata pine [28]. This paper will focus solely on Douglas-fir.

Six models to predict the $DLLBH$ will be discussed in the following chapters. While all focus on predicting $DLLBH$, the two Sections of Chapters 2 and 3 take two different approaches. The first approach, as outlined in Section 2.2, considers an exponential power function with respect to various tree-, stand-, and age[3]-level

[2]Total surface area of branches and bole per unit of land area [26]

[3]Where AGE represents the total age of the subject tree

predictor variables[4]. The second approach, as outlined in Section 2.3, pursues a parameter prediction method, in which the same predictor variables are considered. This approach investigates whether or not the model can be simplified by taking advantage of allometric relationships of $DLLBH$ and DBH, while using simple linear functions of the independent variables in order to estimate the parameters on DBH. The reasoning behind the latter approach is to advocate a parsimonious and biologically meaningful model as opposed to one which simply has good fit statistics, low Akaike information criterion (AIC), etc.

In contrast to other models that have predicted $DLLBH$ ([6], [7], [8]) on either alive **or** dead branches, here we look at both the growth of a knot as a live branch as well as the decrease in size of the knot after death[5]. Branch mortality can often be attributed to crown closure and a lack of light being intercepted by the lower branches [27],[19] , which has created the different ages of mortality for the various densities described in the following sections. Once the branch has died, the stem will grow over the branch at the surface of the tree. As a result, the branch diameter at the tree's surface gradually decreases in size due to water loss, bark loss and branch taper. Not surprisingly, large branches that experienced rapid growth will see the same behavior in death, as the stem encases them at a faster rate [8]. This confounding behavior is the motivation behind the nonlinear approaches outlined later in the paper.

The motivation behind investigating tree-, stand-, and age-level covariates is based on several factors. First, we recognize that $DLLBH$ and DBH have an allometric relationship. Second, this study, as outlined in Section 2.1 is based on spacing trials, and therefore the effects of trees per acre are at the center of the study. While stand level metrics have been used by some and not others[6] [8], [25], the nature of this

[4]All variables are fully outlined in Table 2.1, with tree variables (1-10) and stand variables (11-16) distinguished by a single horizontal line

[5]Prior to branch mortality, the knot retained on the tree is referred to as a sound knot and post mortality knots are referred to as loose knots

[6]Often little or nothing may be known about past stand conditions and genetic composition

study seems to necessitate their use. This is also not the first time the approach of building off of DBH has been used as a base with planting density added; however, the other approach used mixed-models [24], again arguing the importance of the relationship between stem and branch girth. Third, most growth and yield models (FVS, ORGANON, etc) do not rely on AGE; however, the Stand Management Cooperative (SMC) has access to repeated measurements in which AGE can be greatly utilized [16].

1.2 Objectives

There are four main objectives of this paper:

1. Use the multivariable combined exponential power function to describe (model) $DLLBH$ in two steps: First by admitting predictor variables as additional factors in the power function portion and linear terms in the exponential portion. Second, by using DBH as the base factor and estimating the parameters with simple linear functions of tree- and stand- variables.

2. Compare and contrast the outcomes for the two model forms, recommending best modeling strategy for this purpose.

3. Compare the utility of using tree- and stand-level covariates.

4. Demonstrate the use of the model as it relates to forest management by using statistical quality control techniques.

Chapter 2 will fully describe the data, types of models used, and the methods used to fit the models[7]. Chapter 3 reveals the six candidate models, with a section dedicated to a specific summary. Chapter 4 further dissects each model and resulting behavior as it relates to each covariate. Here, a section will point out the strengths and

[7]Additional descriptions of the data can be found in the Appendix

weaknesses of both approaches, followed by practical uses of the model as it relates to statistical quality control. Chapter 5 succinctly concludes all abovementioned objectives of the paper.

Chapter 2

MATERIALS, MODELS AND METHODS

2.1 The Data

Data were available from the Stand Management Cooperative (SMC), an organization developed to synthesize forestry interests from over 40 private companies, universities, and state, federal and provincial agencies. The data are derived from 22 installations from Oregon to British Colombia, east to the Cascade Mountain Range and west to the Pacific Coast. A description of each installation can be found in Appendix Table A.1.

The original goal of these study sites[1] was to assess the effects of planting density on tree and stand development. There were a total of 22 pure Douglas-fir installations used in this particular study, a map of which may be found in Figure 2.1. Within each installation there are a total of six plots representing the following gradient of planting densities: 100 (21 $\times$ 21 ft.), 200 (15 $\times$ 15 ft.), 300 (12 $\times$ 12 ft.), 440 (10 $\times$ 10 ft.), 680 (8 $\times$ 8 ft.), and 1210 (6 $\times$ 6 ft.) trees per acre (TPA) [21][2]. These are *target* densities and do not necessarily reflect the actual *planted* densities. While Washington state law requires more than 100 TPA to be planted after harvest, and 1210 TPA is not seen outside of research plots, these two extrema provide insight into branch development. Figure 2.2 displays the plot-level histograms of branch size by TPA.

---

[1]Known as the Type III installations

[2]This included a total of 16,882 branch measurements

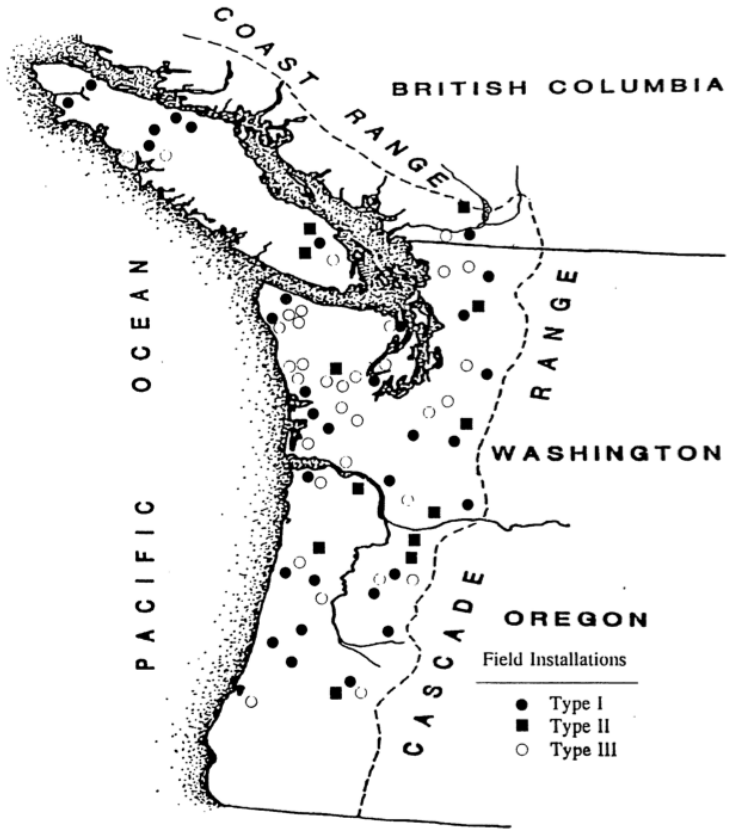

Figure 2.1: SMC Installation Map

Several tree-level variables were measured within each plot and installation, and from those many stand-level metrics were used to describe the stand attributes. A complete description of variables used in this study can be found in Table 2.1, with the basic stand summaries by each variable in Table 2.2. Tree-variables are separated from stand-variables by a horizontal line.

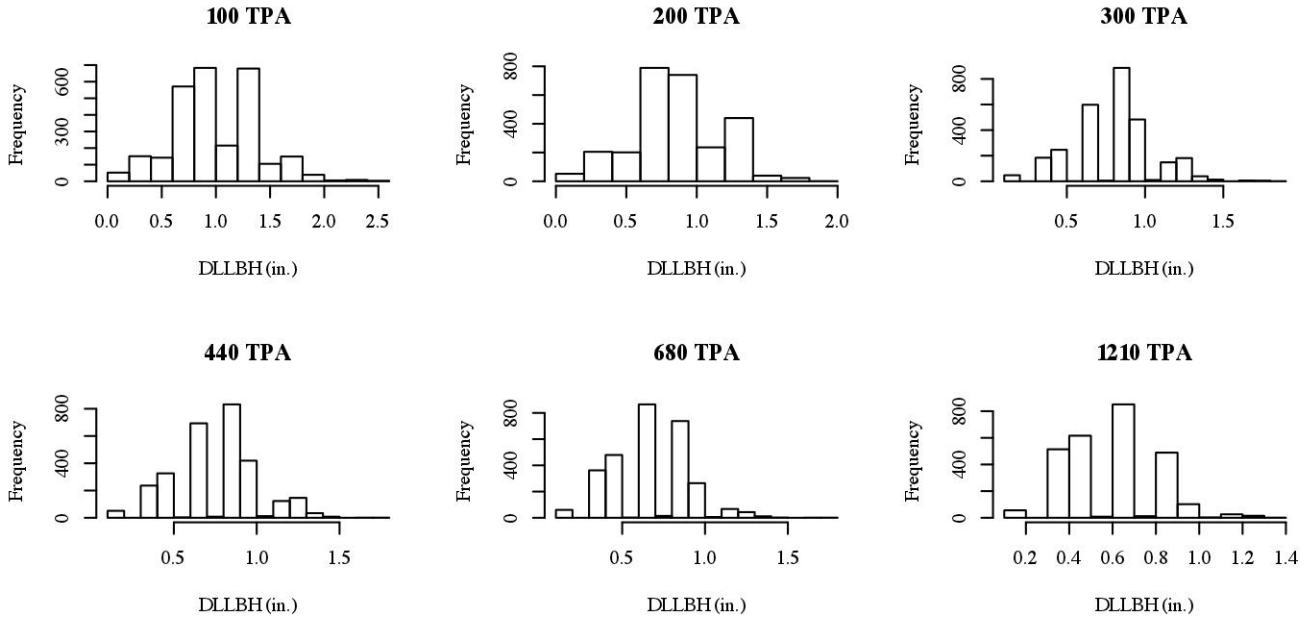

Figure 2.2: Histograms of Branch Sizes by Target Densities

$DLLBH$ was remeasured at various intervals over the past several decades, adhering to the following protocol: 1) Find the first whorl above breast height (4.5 ft.), 2) From the breast height whorl proceed $\frac{1}{2}$ way above to the next whorl as well as $\frac{1}{2}$ below the breast height whorl and measure the $DLLBH$, and 3) Count the number of branches greater than half the size of the $DLLBH$, while recording the status (dead or alive) of the branch.

Table 2.1: Description of Variables

Variable	Description
(1) $DLLBH$	Diameter of the largest limb in the breast height region of the tree (in.)
(2) DBH	Diameter at breast height (in.)
(3) HT	Total height (ft.)
(4) CBH	Height to live crown base (ft.)
(5) HD	Height to diameter ratio (unitless)
(6) CL	Crown length: HT - HCB (ft.)
(7) CR	Crown ratio: 1- $\frac{HCB}{HT}$ (unitless)
(8) BR	Bole ratio: $\frac{HCB}{HT}$ (unitless)
(9) BA_T	Basal area of subject tree ($.005454^{*}DBH^2$) (sq. ft.)
(10) DBH_{REL}	DBH of the subject tree divided by the corresponding stand QMD $\frac{in.}{\sqrt{in.}}$
(11) BA_S	Total basal area of the subject stand (sq. ft.)
(12) QMD	Quadratic mean diameter ($\sqrt{\frac{BA_T}{.005454^{*}n}}$) (in.)
(13) TPA	Trees per acre (actual not targeted)
(14) TPA_0	Trees per acre planted
(15) RD	Curtis' relative density ($\frac{BA_S}{\sqrt{QMD}}$) (ft.^{2}in.$^{-.5}$)
(16) SI_{30}	Site index (average dominant height at 30 years, (ft.))
(17) AGE	Total age of the subject tree (yr.)

As Table A.1 indicates, the branches were remeasured at various stages of development. While having access to truly repeated measurements is the most accurate way in which to predict branch mortality [27], this study does not necessarily imply repeated repeated branch measurements because there is no guarantee the same branches were measured one year to the next. While this is possible, it seems unlikely given the branches were not tagged, measurements were separated by up to four years, and a host of other factors including animal damage, human damage, weather

damage, etc could have caused the subject branch to break and die. However, the trees themselves were remeasured and the data are of a hierarchical nature: branches as subsets of trees, which are subsets of plots, etc.

Table 2.2: Summary Statistics for Covariates

Variable	Mean	Standard Deviation	Minimum	Maximum
$DLLBH$	.7949	.3053	.1000	2.500
DBH	5.215	2.627	.2000	15.40
HT	32.13	14.28	4.700	76.70
CBH	7.520	8.465	.1000	51.60
HD	78.96	20.65	15.52	360
CL	24.61	9.864	1.100	60.70
CR	.8017	.1574	.0426	.9962
BR	.1983	.1574	.0038	.9574
DBH_{REL}	.9938	.2618	.0663	3.997
BA_T	.186	.175	.0002	1.293
BA_S	57.54	45.86	.0191	203.8
QMD	5.271	2.335	.2012	12.48
TPA	382.9	265.8	50.00	1165
TPA_0	404.7	282.8	69.00	1179
RD	23.80	17.58	.0427	80.95
SI_{30}	85.95	11.37	51.00	114.0
AGE	15.09	3.948	7	24

2.2 Type I Models: Combined Exponential Power Function

As previously mentioned, a nonlinear model will be used:

$$\mathbf{DLLBH}_i = g(\mathbf{X}_i; \boldsymbol{\theta_i}) + \boldsymbol{\epsilon}_i, \tag{2.1}$$

where $\mathbf{DLLBH}_i$ is an $n_i \times 1$ vector of observed values based on tree 'i', g can be any nonlinear function, $\mathbf{X}_i$ is any covariate appearing in Table 2.1, $\boldsymbol{\theta_i}$ is an $n_i \times m$ vector of effects, and $\boldsymbol{\epsilon_i}$ is an $n_i \times 1$ vector of errors, which are assumed to independently and identically (normally) distributed with E[$\boldsymbol{\epsilon}$]=0 and Var($\boldsymbol{\epsilon}$)=σ^2 [3].

The combined exponential power function was the platform for model fitting and will represent g in Equation 2.1[3]. The univariate form was taken from the *Biometrics Information Handbook No. 4* [22], and is easily extended to the multivariate form:

$$DLLBH = \alpha \prod_i X_i^{\beta_i} e^{\sum_i \lambda_i X_i}, \tag{2.2}$$

where X_i is as previously defined, and α_i, β_i, and λ_i are parameters estimated using nonlinear least squares. The objective of nonlinear least squares is not unlike that of ordinary least squares, where we wish to minimize the sum of squares of deviations between the recorded values and the predicted values:

$$min(\boldsymbol{\theta_i}) = \sum_i (DLLBH_i - g(\mathbf{X}_i; \boldsymbol{\theta_i}))^2, \tag{2.3}$$

where g is represented by Equation 2.2. Nonlinear least squares was implemented via the statistical program R using the Gauss-Newton algorithm to identify parameter estimates. In order to fit a nonlinear model we need proper starting values, or we will not reach convergence. In order to do this, the linearized form of Equation 2.2 was used:

$$ln(DLLBH) = ln(\alpha) + \sum_i \beta_i ln(X_i) + \sum_i \lambda_i X_i, \tag{2.4}$$

---

[3] An inverse quadratic function was also analyzed, but without improvement on 2.2

again where X_i is as previously defined and α, β, and λ are parameters estimated using ordinary least squares. Once parameters were estimated from Equation 2.4, they were backtransformed and used as initial estimates of the parameters.

Variable selection proceeded in a modified setpwise manner, with DBH being the first variable to enter the model given the known, close relationship to $DLLBH$. Criteria for adding variables involved several steps. First, a ratio of the the observed values and residual values was plotted as a function of the next variable of interest (see Figure 2.3) [3]. The use of residuals in the form of the ratio of observed to predicted rather than the difference was used as it is appropriate for the mutiplicative form of Equation 2.2. If there appeared to be a relationship between the quotient of observed values and predicted values with the covariate of interest, $\frac{y}{\hat{y}}$ was regressed on x_i and added to the model based on the strongest relationship.

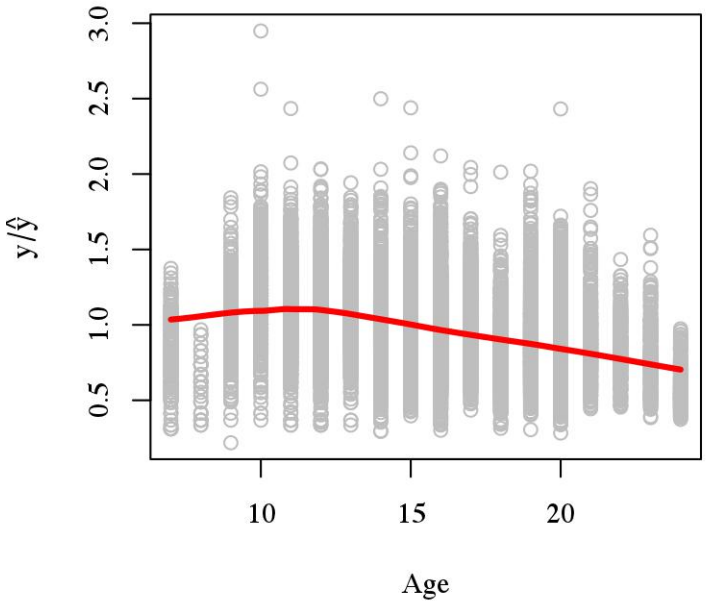

Figure 2.3: Method for Adding Variables

Then, if parameter estimates were significant, the variable would be kept in the model. In many cases the variables maintained statistical significance but did not necessarily produce a 'better' model. The biological interpretability of the estimates was the initial characteristic to determine whether or not the added variable improved the form. Models depicting unreasonable biological behavior were not further considered. For example, a model that produced and exponential increase in $DLLBH$ as the DBH increased does not fit with the known behavior and therefore was eliminated. Second was the amount to which the new variable decreased the residual standard error (RSE). When the added variable failed to reduce the RSE by more than 2% it was not included. Additionally, a correlation matrix[4] was produced in order to check for 'high' correlation (not a universally practiced part of the process), but often useful to further investigate when greater than the absolute value of .99 [3].

[4]Numbers in Figure 2.4 indicate the degree of correlation, with intense blue indicating strong positive correlation and intense red indicating strong negative correlation

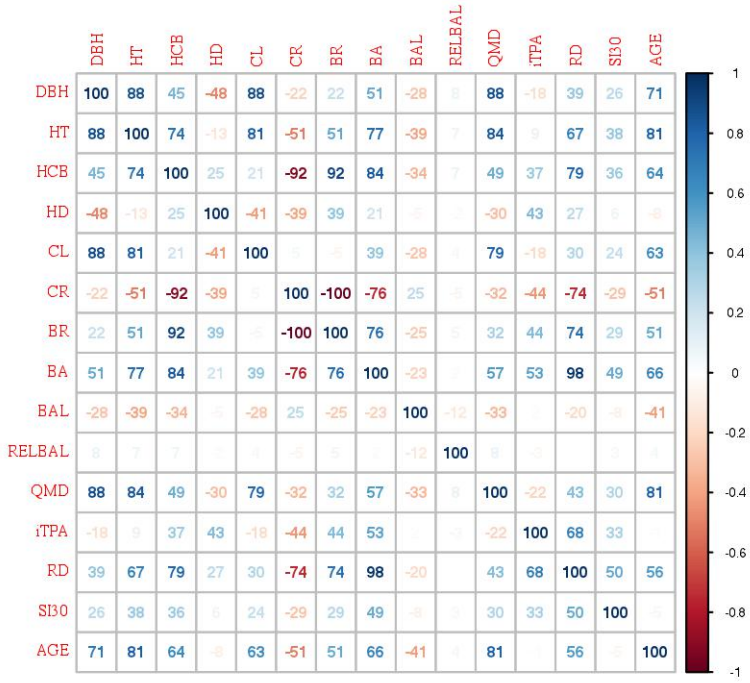

Figure 2.4: Correlation Matrix for all variables considered

Once final model forms were selected, they were dissected in order to observe behavior as each covariate was varied. This process involved breaking each covariate into quintiles and plotting them over all other covariates. In order to check convergence of the parameters, 2 approaches were taken: 1) Starting values for parameter estimates were changed up to an order of magnitude and the model was rerun, and 2) the parameter estimates that the model converged to were then used as the starting values to ensure they converged again to the same values. In addition, the usual diagnostics of the error structure were evaluated, which included the following: Calculating the ratio of the variances of residuals coming from the top 25% and bottom 25% in order to screen for heteroscedasticity, and computing the residual standard error (RSE), mean squared error (MSE), mean absolute error (MAE), mean error (ME) or *bias*, coefficient of determination (r^2), and Akaike information criterion (AIC). These fit

statistics were all calculated as follows:

$$RSE = \sqrt{\frac{\sum_i (y_i - \hat{y}_i)^2}{n-k}} \tag{2.5}$$

$$MSE = \frac{\sum_i (y_i - \hat{y}_i)^2}{n} \tag{2.6}$$

$$MAE = \frac{\sum_i |y_i - \hat{y}_i|}{n} \tag{2.7}$$

$$ME = \frac{\sum_i (y_i - \hat{y}_i)}{n} \tag{2.8}$$

$$r^2 = (COR(y, \hat{y}))^2 \tag{2.9}$$

$$AIC = 2k - 2ln(L), \tag{2.10}$$

where y_i are the observed values, $\hat{y}_i$ are the predicted values, n is the number of elements in the population, k is the number of parameters in the model and L is the maximum value of the likelihood function.

2.3 Type II Models: Parameter Prediction Method

In this section the same function as in Section 2.2 is used, but in this case relationships were sought between the additional covariates and the parameters estimated (α, β, λ), taking advantage of the allometric relationship between tree diameter and branch diameter and thus using DBH as the base covariate. Therefore, the second model is of the form:

$$DLLBH = \alpha(X_i) DBH^{\beta(X_i)} e^{\lambda(X_i) DBH}, \tag{2.11}$$

where α, β, λ represent simple linear forms of the variables in Table 2.1[5], and are estimated in the same manner described in Section 2.2 . This process first involves fitting five separate nonlinear models of the form:

$$DLLBH = \alpha_l DBH_l^{\beta_l} e^{\lambda_l DBH_l}, \tag{2.12}$$

(for l=1,2,3,4,5) based on five relatively equally sized subsections of the data[6]. DBH is broken into quintiles corresponding to the quintiles of the variable of interest, and represents a 5×1 vector of means. Each α_l, β_l, and λ_l are extracted from the five models and plotted against the next covariate of interest, as seen using AGE in Figure 2.5.

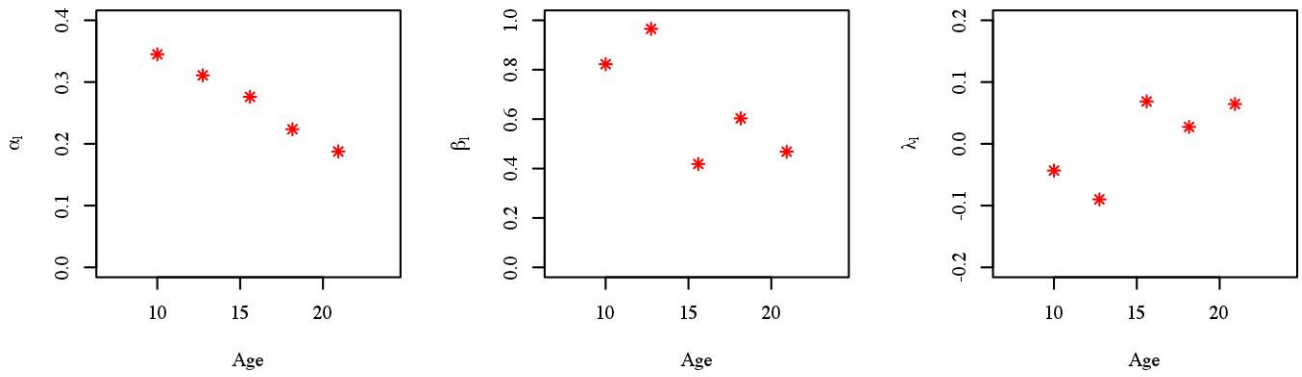

Figure 2.5: Method for Adding Variables via the Parameter Prediction Method

Should there appear to be a trend, simple linear functions are formed:

$$\alpha_l = \alpha_{0j} + \alpha_{1j} X_j \tag{2.13}$$

[5]Excluding DBH

[6]Chosen to produce exhaustive, non overlapping regions over the variable range; however, in some cases quintiles are more exact if the covariate has a finer resolution, e.g. QMD versus AGE.

$$\beta_l = \beta_{0j} + \beta_{1j} X_j \tag{2.14}$$

$$\lambda_l = \lambda_{0j} + \lambda_{1j} X_j, \tag{2.15}$$

where X_j is any covariate in Table 2.1, except for DBH, and the subscripts 0 and 1 represent the intercept and slope, respectively. The original nonlinear function is then refit with the new parameters and compared to the form in Section 2.2 to see whether the new form is simpler and/or captures a larger amount of variation. The same list of error structure diagnostics as listed in Section 2.2 as well as biological interpretability were also used in the selection process.

Chapter 3

RESULTS

In parallel to Chapter 2, results are discussed separately for each modeling process. This involves two sections: 1) the results from the combined exponential power function (Equation 2.2) and 2) the results from the parameter prediction method with DBH base (Equation 2.12). Each section is then further divided into the three model types: First using tree-variables, then adding stand-variables, and finally adding age.

Model results are displayed graphically, in tables and through equations. Independent variables are subdivided into quintiles for full model transparency, and complete lists of all other models can be found in the Appendix A. Each subsection displays the top three models, their associated fit statistics, R^2 values, and AIC values.

3.1 Model Type I: Combined Exponential Power Function

3.1.1 Tree-level variables only

All tree-level measurable variables as well as tree-level derived variables located in Table 2.1 were considered. As mentioned in Chapter 2, a modified stepwise route was taken, with DBH always used in the model so as to preserve the allometric relationship with $DLLBH$. A full list of these models, residual standard errors (RSE), RSE comparisons, as well as important model comments can be found in Table A.3[1]. Table 3.1 lists the top three models, with the model selected as *best*[2] highlighted and

[1]The first model summary table is Table A.3. The first model has the number 1 by it and is just DBH. Move down 1 line to Model 1.1, which says '1, HD' in the 'Variables' column implying DBH and HD. Move down to the highlighted Model 1.14, which says '1.1, BA' implying everything from Model 1.1 and BA. The 'RSE % Decrease' in this row implies the decrease from Model 1.1.

[2]Why the highlighted model is *best* is further explored in Chapter 4

displayed below:

Table 3.1: Summary of Best Tree-Level Based Models

Variables Included	RSE ($in.$)	MSE ($in.^2$)	MAE ($in.$)	ME ($in.$)	R^2	AIC
DBH, HT, CBH	.1729	.0299	.1320	-.0004	.6797	-11,348
DBH, HT, BR	.1735	.0301	.1326	-.0003	.6773	-11,225
DBH, HT, CR	.1741	.0303	.1326	-.0003	.6751	-11,008

Model 3.1 is as follows:

$$DLLBH = \alpha(DBH^{\beta_1} HT^{\beta_2} CBH^{\beta_3}) e^{(\lambda_1 DBH + \lambda_2 HT + \lambda_3 CBH)} \tag{3.1}$$

Figure 3.1 displays the residual diagnostics for Model 3.1, with the physical data overlaid in the background. While the upper tail in the normal Q-Q plot does appear to be skewed, this is to be expected given the sample size.

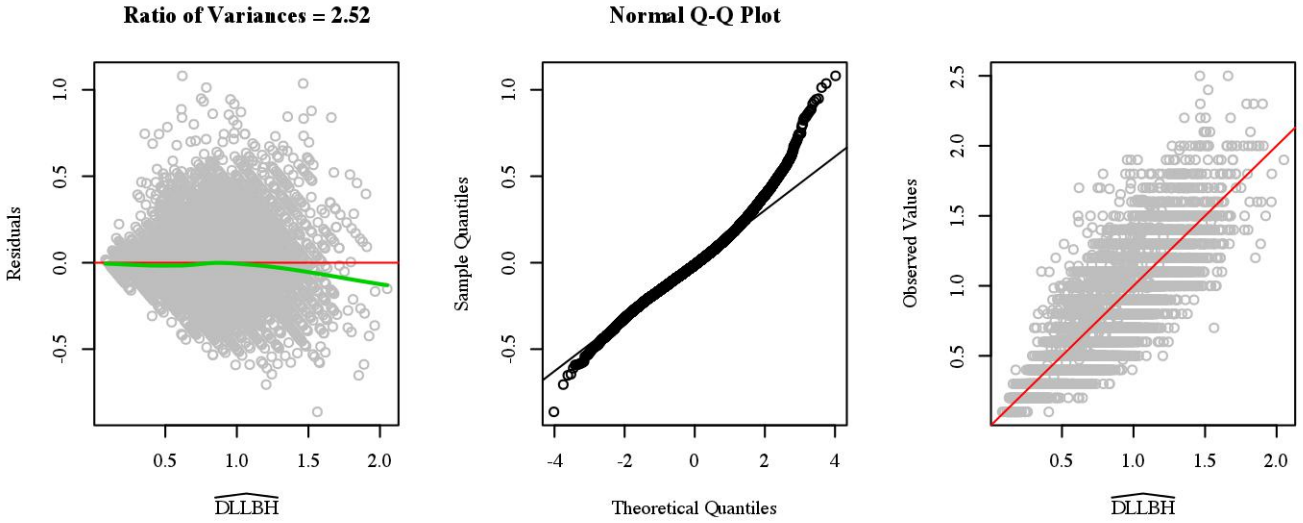

Figure 3.1: Residual plots and analysis for Model 3.1

Table 3.2 displays the parameters and associated standard errors. All parameters were significant at the α=.1 level[3].

Table 3.2: Parameter Estimates and Standard Errors for Model 3.1

Parameter	Estimate	Standard Error
α	.4486	.0310
β_1	.8531	.0232
β_2	-.0756	.0339
β_3	-.1064	.0031
λ_1	.0312	.0035
λ_2	-.0175	.0010
λ_3	.0058	.0005

3.1.2 Tree and stand-level variables only

Model 3.2 does not necessarily improve on Model 3.1 in terms of fit statistics, R^2 or AIC; however, it is important to explore the use of stand level metrics in this process given the Type III installations are in part a study on the effects of spacing. Table A.5 lists RSEs and comments for other candidate models in this section. Table 3.3 lists the top three models with the highlighted model selected as *best*.

[3]t-values and associated p-values are omitted from here on for brevity

Table 3.3: Summary of Best Tree-, Stand-Level Based Models

Variables Included	RSE ($in.$)	MSE ($in.^2$)	MAE ($in.$)	ME ($in.$)	R^2	AIC
DBH, HD, BA_S	.173	.0299	.1313	0	.6790	-11,314
DBH, TPA_0, HD	.1782	.0317	.1367	.0005	.6596	-10,320
DBH, TPA_0, HT, CBH	.1712	.0293	.1308	-.0004	.6959	-11,689

The covariates accounted for similar amounts of variation, but it took four variables instead of three in two of the models to do so. Model 3.2 is as follows:

$$DLLBH = \alpha(DBH^{\beta_1} HD^{\beta_2} BA_S^{\beta_3}) e^{(\lambda_1 DBH + \lambda_2 HD + \lambda_3 BA_S)} \tag{3.2}$$

Figure 3.2 displays the residual diagnostics with the data overlaid in the background. Again it appears that the the upper tail of the residuals is skewed, but this should not be a large problem given the sample size.

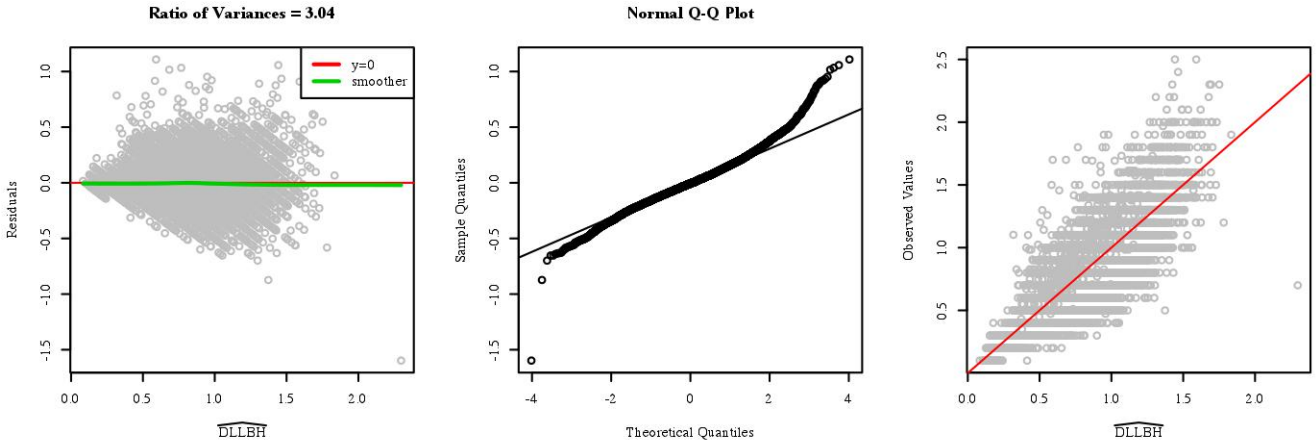

Figure 3.2: Residual plots and analysis for Model 3.2

Table 3.4 displays the parameter estimates and corresponding standard errors for

Model 3.2, with all parameter estimates significant at the α=.001 level.

Table 3.4: Parameter Estimates and Standard Errors for Model 3.2

Parameter	Estimate	Standard Error
α	6.176	9.359e-01
β_1	6.201e-01	1.406e-02
β_2	-2.580e-02	2.231e-03
β_3	-6.590e-01	4.575e-02
λ_1	2.175e-03	6.280e-04
λ_2	-2.041e-02	4.384e-03
λ_3	-2.407e-03	9.594e-05

3.1.3 Tree- and stand-level variables, including age

The *best* model in terms of fit statistics, R^2, and AIC that also maintained logical biological behavior was a function of *(DBH, AGE, TPA_0, HD)*. In addition, the *best* model when only considering fit statistics, R^2, and AIC was a function of *(DBH, AGE, TPA_0, HT, CBH)*. However, given Ockham's razor [3] for model parsimony it makes more sense to use a simpler model with the independent variables DBH, AGE, and TPA_0 that still behaves logically as opposed to adding other factors for minimal gains in fit statistics. None of these are derived variables, they are easily measured, and speak towards the allometric relationship as well as the direct competition that captures the confounding behavior of DLLBH as it developes. Furthermore, these variables will provide a parallel with Subsection 3.2.3 for comparison between the two modeling techniques. Table A.6 displays all researched models, while Table 3.5 highlights the top three consisting of the abovementioned variables along with their associated fit statistics, R^2 and AIC values.

Table 3.5: Summary of Best Tree- and Stand-Level Based Models, Age Included

Variables Included	RSE ($in.$)	MSE ($in.^2$)	MAE ($in.$)	ME ($in.$)	R^2	AIC
AGE, DBH, TPA_0	.1663	.0277	.1261	.0001	.7033	-12,650
AGE, DBH, TPA_0, HD	.1617	.0262	.1224	-.0003	.7195	-13,593
AGE, DBH,TPA_0, HT, CBH	.1589	.0252	.1198	-.0002	.7292	-14,178

Model 3.3 is therefore of the form[4]:

$$DLLBH = \alpha(DBH^{\beta_1} TPA_0^{\beta_2}) e^{(\lambda_1 TPA_0 + \lambda_2 AGE)} \tag{3.3}$$

Figure 3.3 displays the graphical residual analysis for Model 3.3, where we still see skewness in the upper tail, which is not uncommon given the sample size of this study.

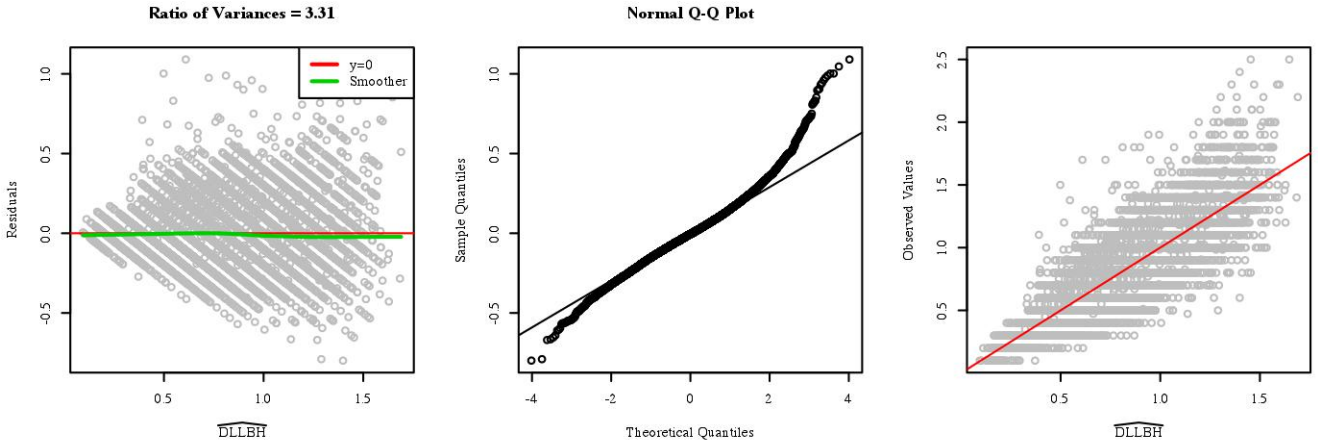

Figure 3.3: Residual plots and analysis for Model 3.3

[4]It should be noted that AGE^{β_3} and $e^{\lambda_3 DBH}$ were not significant and dropped from the model

Table 3.6 lists all parameter estimates and their associated standard errors. All estimates were significant at the α=.001 level.

Table 3.6: Parameter Estimates and Standard Errors for Model 3.3

Parameter	Estimate	Standard Error
α	1.278e+00	3.572e-02
β_1	-5.320e-02	6.218e-04
β_2	-1.335e-01	5.761e-03
λ_1	-5.467e-05	1.697e-05
λ_2	7.076e-01	4.881e-03

3.2 Model Type II: Parameter Prediction Method

3.2.1 Tree-level variables only

DBH was used as the sole base variable with other tree variables entering the model as linear functions of the parameters. The results of the simple functions representing the α, β, and λ parameters are displayed in Table A.7[5]. All significant linear models were then used as parameter estimates with only DBH as the base variable. A complete list of these models, RSEs, and comments can be found in Table A.8[6]. A brief description of the top three can be found below.

Table 3.7 lists the top three candidate models. While the model forms that included HT had better fit statistics, the behavior of $DLLBH$ with respect to DBH became illogical because it increased without bound. In reference to Table A.7 we see that in exploring functions of HT, it was only the $\alpha(HT)$ section of Equation 2.11 that was statistically significant. When $\alpha(HT)$ was substituted for $\alpha(BR)$, the linear

[5]Added variables in the table represent significance at $\alpha = .01$

[6]Other tree-level variables from Table 2.1 that did not have a statistically significant parameter estimates were omitted from the table

functions of BR in the power ($DBH^{\beta(BR)}$) and exponential ($e^{\lambda(BR)DBH}$) sections of the model were unable to compensate, which caused the uncontrollable growth in $DLLBH$. Similarly, if $\alpha(HT)$ was used without variable exponents on DBH the model behaved illogically. Therefore, even though the use of HT as a variable parameter on DBH improved the fit statistics of the model, this was not enough justification to override the established relationship between $DLLBH$ and DBH, which is that $DLLBH$ should not increases unbounded.

Table 3.7: Summary of Best Tree-Level Based Models Using Parameter Prediction

Variables Included	RSE ($in.$)	MSE ($in.^2$)	MAE ($in.$)	ME ($in.$)	R^2	AIC
DBH, BR	.1913	.0366	.1457	0	.6074	-7,918
DBH, BR, HT	.1781	.0317	.1360	-.0006	.6600	-10,344
DBH, HT	.1869	.0349	.1447	-.002	.6263	-8,717

The best tree-variable model used a linear functions of BR (see Table A.9 for BR quintile breakdown) to estimate the parameters for $DLLBH$ as a a nonlinear function of DBH[7]. Model 3.4 is as follows:

$$DLLBH = (\alpha_{08} + \alpha_{18}BR)DBH^{(\beta_{08}+\beta_{18}BR)}e^{DBH(\lambda_{08}+\lambda_{18}BR)} \tag{3.4}$$

Figure 3.4 displays basic residuals plots, and similar to previous models there appears to be skewness in the upper tail:

[7]In order to be consistent with the the 'ij' subscripts for this section, the 'i' subscript is always be denoted by 0 or 1, for slope and intercept, respectfully. In addition, the j subscript will refer to the order in which the variable occurs in Table 2.1

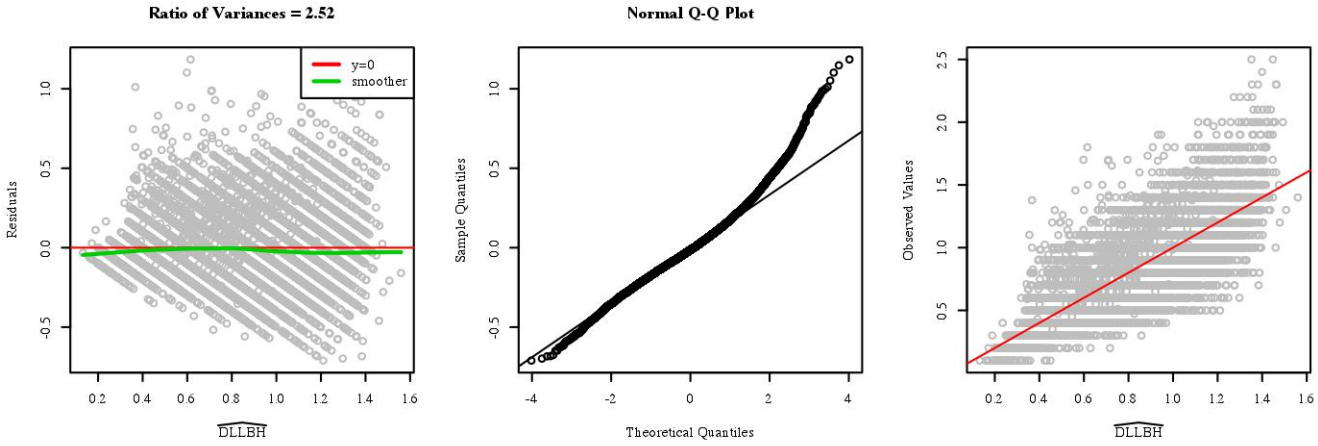

Figure 3.4: Residual plots and analysis for Model 3.4

Table 3.8 lists the parameter estimates from Model 3.4, with accompanying standard errors. All parameter estimates were significant at minimum α=.001.

Table 3.8: Parameter Estimates and Standard Errors Model 3.4

Parameter	Estimate	Standard Error
α_{08}	.3719	.0057
α_{18}	-.0732	.0279
β_{08}	.7685	.0207
β_{18}	-1.545	.0946
λ_{08}	-.0475	.0036
λ_{18}	.2997	.0159

3.2.2 Tree- and stand-level variables only

A variety of tree- and stand-level metrics were used in order to produce a parameter prediction model containing covariates of both varieties. The results of the linear functions of stand-level metrics can be found in Table A.10 with all added variables

significant at α=.1[8]. For a full list of models with RSEs and comments see Table A.13, and for the RD quintile breakdown see Table A.12. The highlighted model in Table 3.9 is the following nonlinear function of DBH with parameters estimated through linear functions of RD. Model 3.5 is as follows:

$$DLLBH = (\alpha_{115})DBH^{(\beta_{015}+\beta_{115}RD)}e^{DBH(\lambda_{015}+\lambda_{115}RD)} \tag{3.5}$$

Table 3.9: Summary of Best Tree-, Stand-Level Based Models Using Parameter Prediction

Variables Included	RSE ($in.$)	MSE ($in.^2$)	MAE ($in.$)	ME($in.$)	R^2	AIC
DBH, RD	.1823	.0332	.1378	-.0001	.6436	-10,320
DBH, HT, RD	.1736	.0301	.1319	-.0002	.6768	-11,202
DBH, TPA_0, HT, RD	.1773	.0314	.1361	-.0013	.6632	-10,495

Figure 3.5 displays residual diagnostics, where again the upper tail is skewed:

[8]This is a looser tolerance than Subsection 3.2.1 because *none* of the stand variables would have been considered if it was tighter, which may imply stand variables have a lesser affect as variable exponents. It should also be noted that using a looser tolerance in Subsection 3.2.1 does not change those results

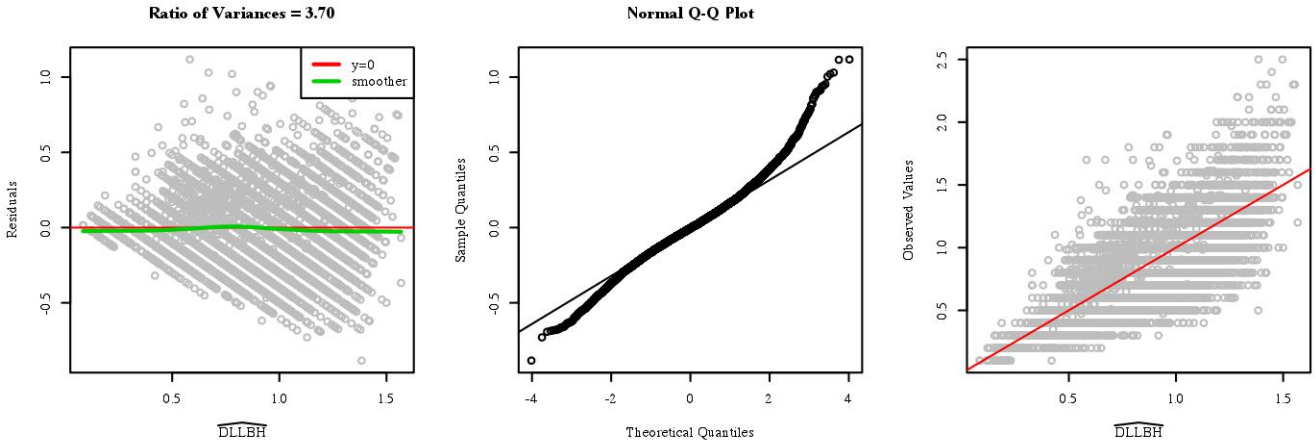

Figure 3.5: Residual plots and analysis for Model 3.5

Table 3.10 lists the parameters associated with Equation 3.5 (all parameters were significant at the α=.001 level):

Table 3.10: Parameter Estimates and Standard Errors for Model 3.5

Parameter	Estimate	Standard Error
α_{015}	0.3451041	0.0033188
β_{015}	0.8716407	0.0160927
β_{115}	-0.0139211	0.0004466
λ_{015}	-0.0527322	0.0034321
λ_{115}	0.0022068	0.0001205

As with the tree-variables only model, HT could have been added to Equation 3.5, and while the RSE would decrease (see Table A.13), the model would not have been useful because the resulting model exhibited an exponential increase in the global behavior of $DLLBH$ as DBH increased; clearly not consistent with known branch shrinkage post mortality.

3.2.3 Tree- and stand-level variables, including age

The final approach involved including AGE as a linear function on DBH in conjunction with tree and stand variables. As seen in Subsection 3.1.3, AGE improved the overall fit statistics of the model (Model 3.3).

Table 3.11: Summary of Best Tree- and Stand-Level Based Models, Age Included Using Parameter Prediction

Variables Included	RSE ($in.$)	MSE ($in.^2$)	MAE ($in.$)	ME($in.$)	R^2	AIC
DBH, AGE, RD	.1627	.0265	.1220	-.0002	.7162	-13,398
DBH, AGE, TPA_0	.1672	.0280	.1264	-.0006	.7001	-12,465
DBH, AGE, BR	.1749	.0306	.1316	-.0002	.6719	-10,950

Model 3.6 is of the form:

$$DLLBH = (\alpha_{017} + \alpha_{117}AGE)DBH^{(\beta_{015}+\beta_{115}RD)}e^{(\lambda_{115}RD)DBH}, \tag{3.6}$$

where $e^{(\lambda_{015})}$ was not significant[9]. The RSE was .1627, which was less than the Model 3.3 (Subsection 3.1.3), which included DBH, AGE, and TPA_0. Figures 3.6 displays the residual diagnostics, again with skewness in the upper tail.

[9]A table of the simple functions of AGE for α, β, and λ was omitted, given the $\alpha(AGE)$-estimate was the only significant portion, and the quintile breakdown of AGE may be found in Table A.14

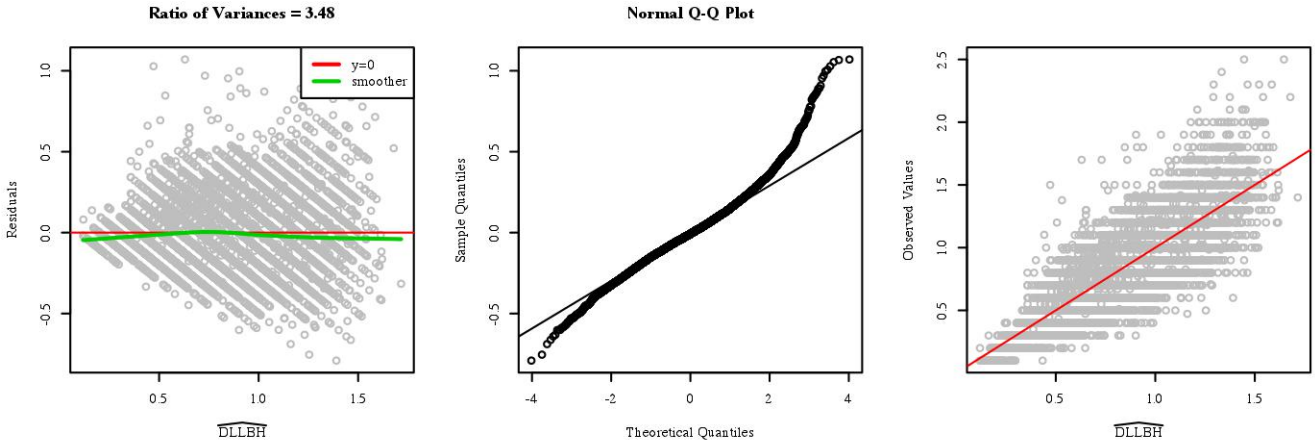

Figure 3.6: Residual plots and analysis for Model 3.6

Table 3.12 displays the parameter estimates and associated standard errors for Model 3.6:

Table 3.12: Parameter Estimates and Standard Errors for Model 3.6

Parameter	Estimate	Standard Error
α_{017}	.4385	.0033
α_{117}	-.0108	.0001
β_{015}	.7997	.0051
β_{115}	-.0086	.0003
λ_{115}	.0011	6.813e-05

3.3 Summary

Table 3.13 describes the final forms for both Model Types I and II. All numerical parameter estimates are displayed for a complete summary:

Table 3.13: Final Model Forms for Types I and II

Model	
Type I	Form
3.1	$DLLBH = .4486(DBH^{(.8531)}HT^{(-.0756)}CBH^{(-.1964)})e^{((.0312)DBH-(.0175)HT+(.0058)CBH)}$
3.2	$DLLBH = 6.176(DBH^{(.6201)}HD^{(-.0258)}BA_S^{(-.659)})e^{((.002175)DBH-(.02041)HD-(.002407)BA_S)}$
3.3	$DLLBH = 1.278(DBH^{-.05320}TPA_0^{-.1335})e^{(-5.467e-05)TPA_0+.7076AGE)}$
Type II	
3.4	$DLLBH = (.371916 - .073274BR)DBH^{(.768488-1.545199BR)}e^{(-.047563+.2997BR)DBH}$
3.5	$DLLBH = (.3451041)DBH^{(.8716407-0.0139211RD)}e^{(-0.0527322+.0022068RD)DBH}$
3.6	$DLLBH = (.4385 - .0108AGE)DBH^{(.7997-(.0086)RD)}e^{(.0011RD)DBH}$

Table 3.14 is a side-by-side comparison of how the two modeling approaches differed in RSE and AIC based on tree-, stand-, and age- independent variables.

Table 3.14: RSE, AIC for Final Models of Types I and II

	Type I	RSE	AIC	Type II	RSE	AIC
Tree-	3.1	.1729	-11,348.12	3.4	.1913	-7,917.631
Tree-, Stand-	3.2	.173	-11,314.41	3.5	.1823	-9,554.712
Tree-, Stand-, Age-	3.3	.1663	-12,650.15	3.6	.1629	–13,398.16

Chapter 4
DISCUSSION

After close examination of fit statistics, the next important step was to determine whether or not the models made sense biologically. This process may be best completed by a close examination of $DDLBH$ behavior with respect to each covariate in the model. Therefore, each variable was broken into quintiles and $DLLBH$ was plotted over the remaining k-1 variables, separately for each quintile of the k^{th} variable. In other words, one variable was held constant to five points that were the means of each quintile. Then, one variable was allowed to vary (always displayed on the x-axis). Finally, in the vase of 2+ variables, the values for the third variable were generated by localized smoothing. For example, in Figure 4.1 values for CBH were generated via localized smoothing: CBH as a 'function' of DBH based on the quintile subsets of HT.

This was done to make model behavior more transparent, as well as show how $DLLBH$ behaves at various levels of tree and stand attributes. For the preliminary biological rational the plots do not exceed 10% of the maximum values in the dataset. While $DLLBH$ behaved logically well beyond 10% of the maximum values for the models, users of the models are encouraged to use caution when making extrapolations of any magnitude.

4.1 Behavior of Combined Exponential Power Models

4.1.1 Tree-level variables only

In Figure 4.1 we can see that the behavior of $DLLBH$ as DBH increases based on the quintiles of HT is biologically reasonable. At the mean of the lowest quintile of

HT (13.3 ft.), we see the smallest $DLLBH$ sizes.

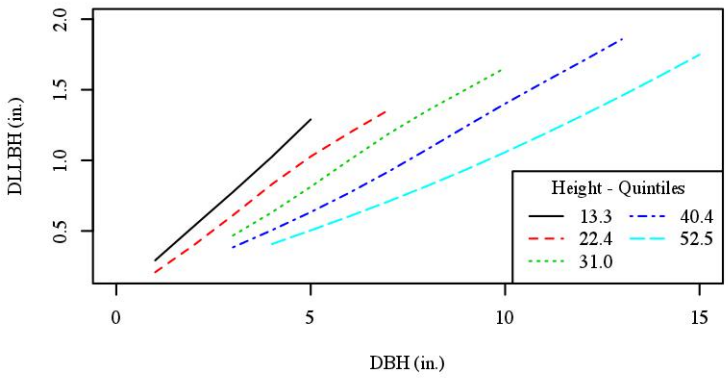

Figure 4.1: Predictions for Model 3.1: HT over DBH

Perhaps more interestingly, Figure 4.2 displays the behavior of $DLLBH$ with respect to HT based on mean quintiles of DBH. As expected, the highest mean DBH quintile produces the largest $DLLBH$ sizes, while consistently decreasing with gains in HT.

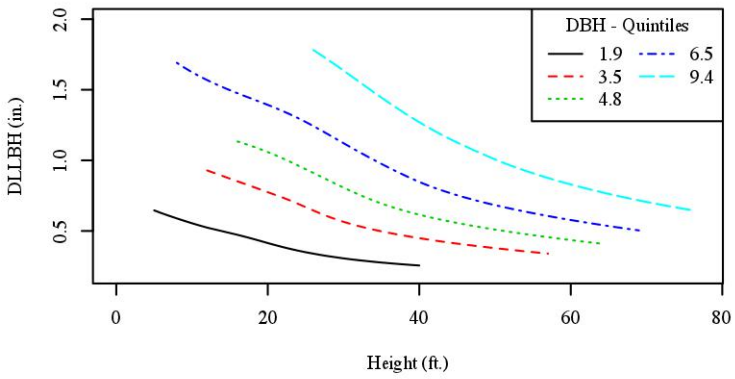

Figure 4.2: Predictions for Model 3.1: DBH over HT

Lastly, Figure 4.3 displays the behavior of $DLLBH$ with respect to gains in CBH based on mean DBH quintiles. The results are easily interpretably from a biological standpoint: Greater stem sizes produce greater branches. Furthermore, as the crown recedes and CBH approaches HT, $DLLBH$ should consistently decrease.

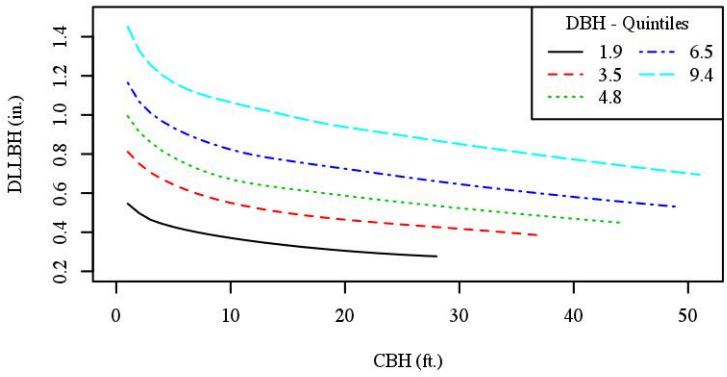

Figure 4.3: Predictions for Model 3.1: DBH over CBH

4.1.2 Tree- and stand-level variables

Figures 4.4, 4.5 and 4.6 display the behavior of $DLLBH$ based on quintile subsets of each variable. Figure 4.4 shows how $DLLBH$ behaves with respect to HD as DBH increases. Again, we expect $DLLBH$ to increase with increasing DBH to some extent, but to decrease beyond a certain point. When looking at the quintiles of HD, we can see the rational behavior of the model. The top line, representing the lowest mean HD quintile (58) and thus the largest DBH (or widest spacing) produces the largest branch diameters. Similarly, the lowest HD produces the smallest branch sizes.

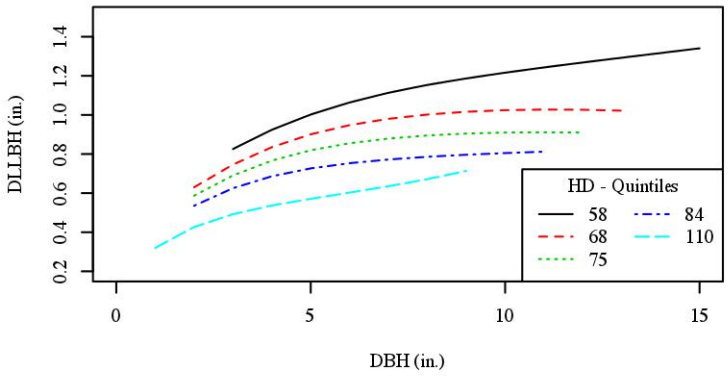

Figure 4.4: Predictions for Model 3.2: HD over DBH

Figure 4.5 displays the behavior of $DLLBH$ with respect to as BA_S based on the quintiles of HD. We expect the highest HD to produce the lowest $DLLBH$ sizes and the lowest HD measurements to produce the largest $DLLBH$ sizes as the BA_S increases, which is clearly indicated in the figure. The biological consistency is therefore preserved.

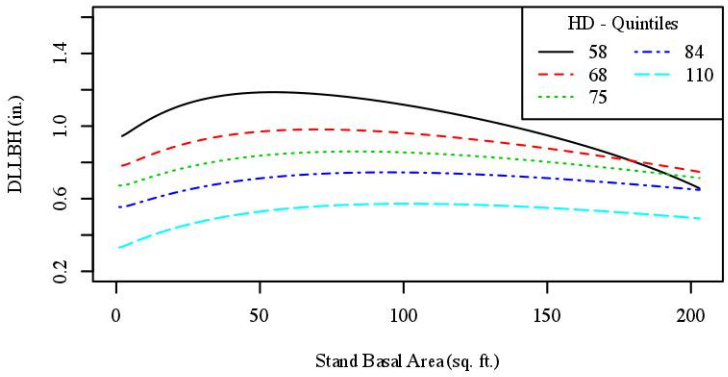

Figure 4.5: Predictions for Model 3.2: HD over BA

The final phase of dissecting the model behavior is to look at how $DLLBH$ changes in relationship to BA_S based on DBH quintiles. The highest quintile average for DBH produces the largest $DLLBH$, which is consistent biologically as well as with Figure 4.6.

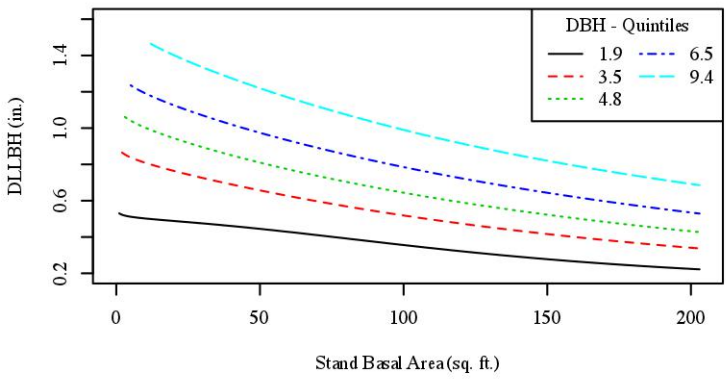

Figure 4.6: Predictions for Model 3.2: DBH over BA

4.1.3 Tree- and stand-level variables, including age

Figures 4.7, 4.8 and 4.9 display the behavior of $DLLBH$ based on quintile subsets of each variable. One might argue that Figure 4.7 is the most easily read $DLLBH$ projection thus far, as we can now view branch development over time instead of using surrogates for time; however, both approaches are biologically relevant and simply display different viewpoints. Though some may wish to see how $DLLBH$ behaves as AGE increases, others may be more interested in the more 'allometric' display, which would show how $DLLBH$ changes with regard to DBH, for example.

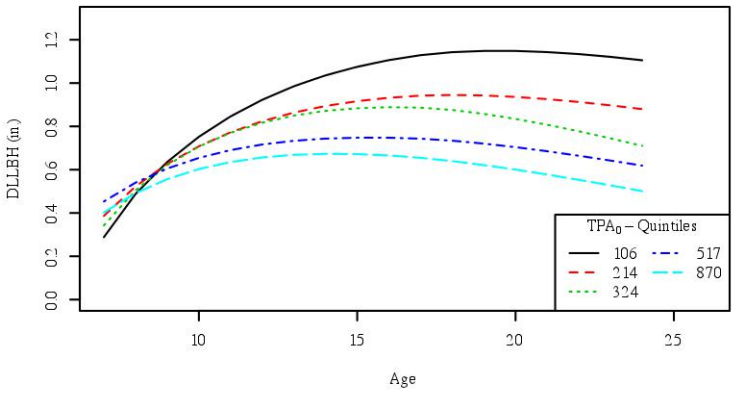

Figure 4.7: Predictions for Model 3.3: TPA_0 over Age

In addition, the highest mean DBH quintile (9.4 inches) produces the largest $DLLBH$ sizes while simultaneously showing the most drastic decrease (roughly .7 inches), as displayed in Figure 4.8.

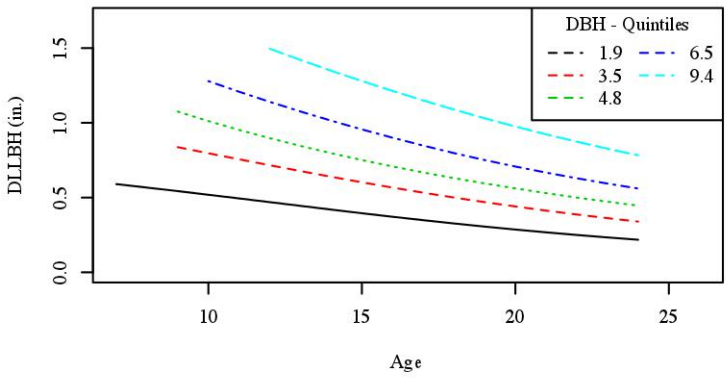

Figure 4.8: Predictions for Model 3.3: DBH over Age

Lastly, Figure 4.9 displays how $DLLBH$ behaves with respect to TPA_0. As expected, the highest mean DBH quintile reflects the largest $DLLBH$ and vice versa.

The lowest mean DBH quintile produces what appears to be little or no change in $DLLBH$ given a low DBH is indicative of a young tree in which the branches are for the most part still alive.

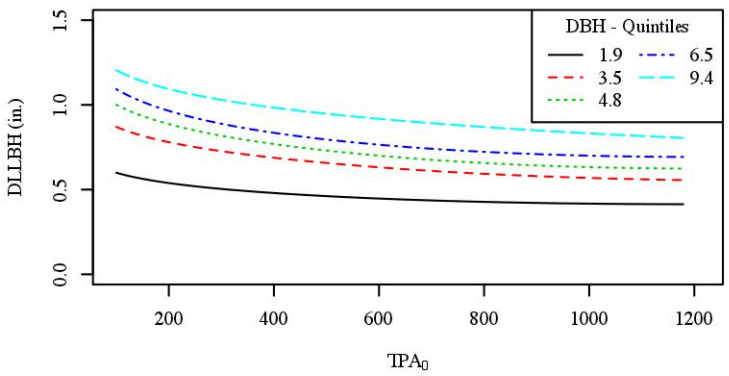

Figure 4.9: Predictions for Model 3.3: DBH over TPA_0

4.2 Behavior of the Parameter Prediction Models

The same approach that was taken in Section 4.1 was used in Section 4.2: Each covariate was dissected into quintals and $DLLBH$ was plotted over the remaining k-1 variables, separately for each quintile of the k^{th} variable.

4.2.1 Tree-level variables only

Figure 4.10 displays the behavior of $DLLBH$ as DBH is broken into quintile subsets and plotted over BR. It is not unreasonable to assume that the closer the BR is to one, that either the tree is older *or* has undergone more severe competition. Therefore, we expect $DLLBH$ to be decreasing along the BR-axis. In addition, the largest $DLLBH$ size is associated with the highest mean quintile of DBH (9.4 inches) and the lowest $DLLBH$ size is associated with the lowest mean DBH quintile (1.9 inches). Though the lowest mean DBH quintile line crosses the four larger quintile

lines, this is expected given that it represents a younger tree in which the branch shrinkage due to mortality is less pronounced than the older trees.

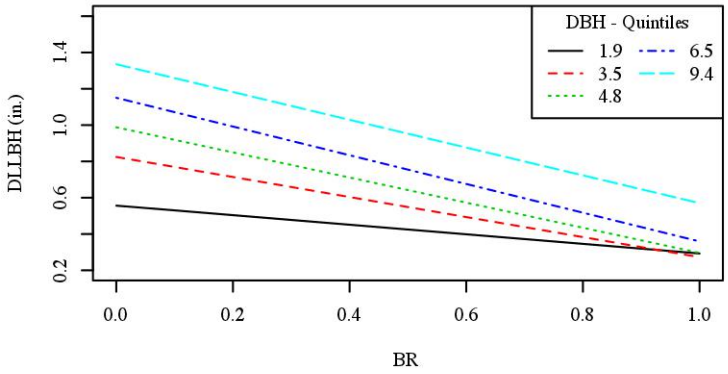

Figure 4.10: Predictions for Model 3.4: DBH over BR

4.2.2 Tree- and stand-level variables

Figure 4.11 displays the behavior of $DLLBH$ with respect to RD based on the quintile subsets of DBH. The model projections are logical: The highest mean DBH quintile (9.4 in.) is associated with the greatest $DLLBH$ size and conversely the lowest mean DBH quintile (1.9 in.) is associated with the smallest $DLLBH$ size. The lowest mean DBH quintile intersects the other lines, again because such a small diameter is associated with young trees that have not responded as strongly to competition.

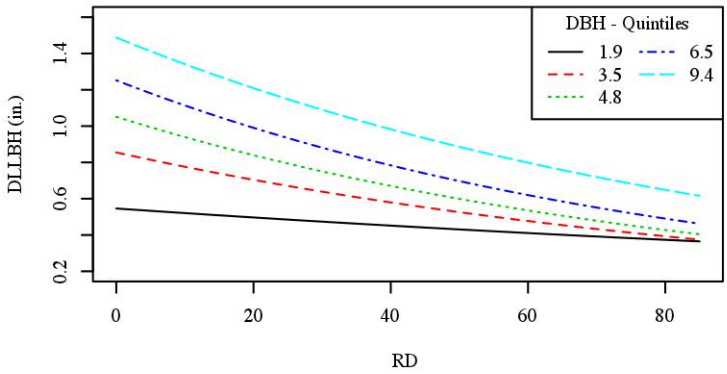

Figure 4.11: Predictions for Model 3.5: RD over DBH, DBH over RD

4.2.3 Tree- and stand-level variables, including age

The advantage to Subsection 4.2.3 is that the same number of variables depict accurate behavior with better fit statistics and a simpler overall model form, while at the same time preserving the basic variable allometric relationship between $DLLBH$ and DBH. The parsimonious nature of Model 3.6 should be considered to be superior quality to its analogue (Model 3.3). Thus, Model 3.6 is the top choice to predict $DLLBH$ in young, Douglas-fir trees.

Figure 4.12 displays the behavior of $DLLBH$ with respect to AGE based on subsets of DBH. When DBH is broken down by quintiles, the larger stems produce larger branches that display the greatest variation in size as AGE progresses. The converse of this holds true for the lowest DBH quintile.

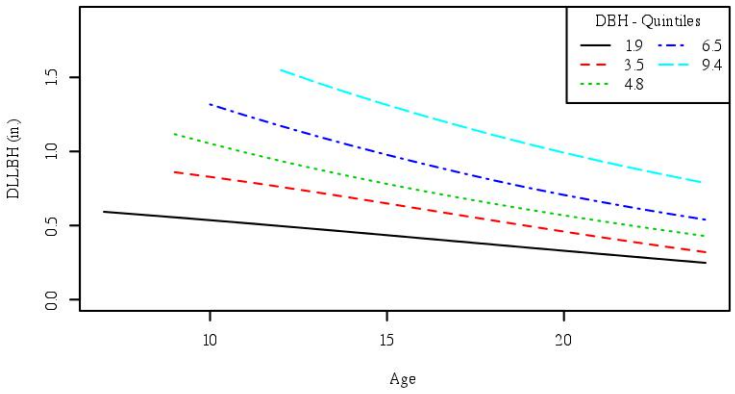

Figure 4.12: Predictions for Model 3.6: DBH over Age

Figure 4.13 displays the behavior of $DLLBH$ with respect to RD based on subsets of DBH. The behavior is again biologically consistent, as the lowest mean DBH quintile is associated with the smallest $DLLBH$ projections and $DLLBH$ consistently decreasing with increasing RD.

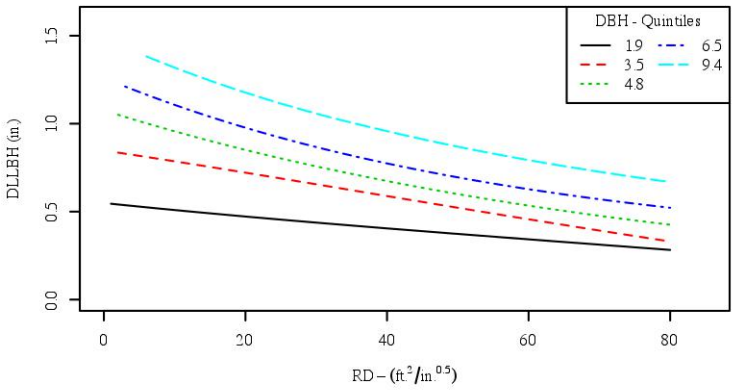

Figure 4.13: Predictions for Model 3.6: DBH over RD

Figure 4.14 depicts the behavior of $DLLBH$ as RD increases based on quintile

subsets of AGE. This particular interaction plot may be most confusing to interpret, but makes sense. For the first four mean AGE quintiles (9-17.5), $DLLBH$ increases, while decreasing along the RD-axis. Therefore, branches are still growing up until around 17.5 years, but still decreasing with increasing RD. However, the largest mean quintile (23.5 years) then shows a dramatic decrease in $DLLBH$, because on average most of the branches have died thus bringing the overall $DLLBH$ size down.

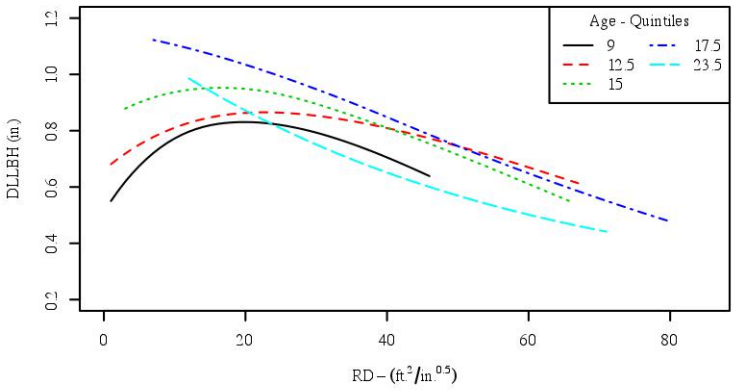

Figure 4.14: Predictions for Model 3.6: AGE over RD

4.3 Comparing Modeling Methodologies

Model Types I and II worked well at modeling $DLLBH$. Both had comparable results in terms of the fit statistics, R^2 values, AIC values and biological realism. However, several variables used in Model Type I were not significant as linear functions, and thus applicable to be used as parameter predictors in Model Type II. This may be in part due to the key allometric relationship between $DLLBH$ and DBH. Using DBH as the sole base variable allows for the power and exponential components of the model to capture the competition aspects of the stands and control the curve shape in a more parsimonious manner than by simply adding more base variables (factors). Table 4.1 is a summary of variables used in both model types:

Table 4.1: Variable Summary for Model Type I and II

	Model	Type I	Model	Type II
Tree	3.1	*DBH, HT, CBH*	3.4	*DBH, BR*
Tree, Stand	3.2	*DBH, HD,* BA_S	3.5	*DBH, RD*
Tree, Stand, Age	3.3	DBH, AGE, TPA_0	3.6	DBH, AGE, RD

When examining tree-variables to be added for parameter prediction, HD was not significant in any of the linear (slope) forms of the parameter functions, and HT was only significant in the intercept portion (Table A.7). Interesting, BR was significant in all three terms and is essentially an interaction between HT and CBH. In a different respect, RD was not significant in either the power or exponential components of Model 3.2 and 3.3, while it was the best parameter predictor for Model 3.5 and 3.6.

The parameter prediction method simplified all three different forms of the model, which is to be expected given the allometric relationship between $DLLBH$ and DBH. While the same number of variables were used in the age-based models, Model 3.6 is simpler than Model 3.3 due to the fact that there were fewer factors in the power and exponential sections. Furthermore, Model 3.6 has the best fit statistics.

Model 3.6 is arguably the best model out of the six that were discussed in the previous sections. In addition to the parsimonious and well behaved nature of the model, it used three basic measurements, DBH, AGE, and RD while preserving the basic variable allometric relationship: $Y = \alpha X^{\beta} e^{\lambda X}$. Nonetheless, the behavioral interpretation of $DLLBH$ also remains intact when metrics such as HT, CBH, or BR are used. As discussed in Section 4.2, BR can be used to gauge both AGE and a density metric. Logically, as AGE increases CBH approaches HT depending on the stand density. A similar argument can be made for other derived variables such as HD in terms of AGE and what actually determines stem form, that is, density in the absence of genetic information. So while Models 3.1-3.4 all display reasonable

biological behavior and are easily interpretable without direct age measurements, those with AGE did outperform them in fit statistics, R^2 values, and AIC values. Therefore, while the other models were biologically rational with good fit statistics, the simplest model accounting for most variation while maintaining biological realism is the top choice.

4.4 Management Implications: Process Capability Analysis

As previously mentioned, the pacific northwest has seen a decline in the quality of timber for several decades, and as a result, purchasers as well as suppliers may desire tools to improve their ability to assess whether or not the product is conforming to desired needs. Furthermore, it is essential to link how the stand is conforming to any number of specifications in the tree-to-log-to-product value chain. The process, known as statistical quality control (SQC), is used in many manufacturing processes where one samples a product to assess whether or not it is meeting some desired property [9]. In this study, the idea is to sample $DLLBH$ and assess whether or not it is meeting standards for acceptable lumber grades. This sample can then be used in two different contexts, both of which are discussed below.

One comparison can be of the selected sample to prior samples, of which there is a known distribution. For example, with a normal distribution one can use measures of central tendency (μ, etc.) and dispersion statistics (σ, etc.) in order to create general bounds on conformance [5], [9]. While this may often include upper and lower bounds, this particular study would only warrant upper limits and may be set by the management objectives[1]. The upper limit is defined by: Upper Limit (UL)=μ+3σ. Similarly, one could express the product capability as a percentage falling outside prior specifications for the goods: C_p=$\frac{UL}{3\sigma}$.

The second comparison could be to see how well the sample conforms to *established*

[1]Upper limits on $DLLBH$ are only considered due to the fact that small branches do not affect the *quality* in the same manner

specifications, as indicated by scientists, purchasers, suppliers, etc. Where these two approaches differ is that one assumes a distribution to create bounds and the other uses prior specifications to mark cut off points. The latter will considered henceforth.

Figure 4.15 displays an a 'predicted' cumulative distribution, the values of which are derived from a model[2] in order to find what percentage of trees do not meet specifications based on $DLLBH$, say 1 inch. Figure 4.15 shows that globally it appears to be roughly 21%.

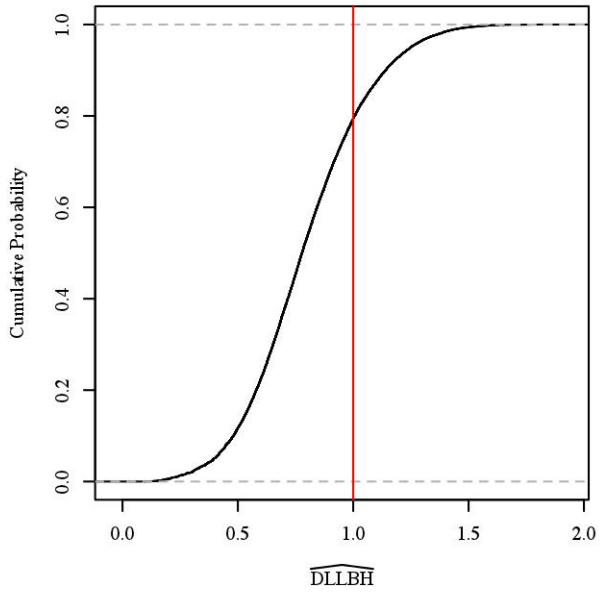

Figure 4.15: Empirical Cumulative Distribution Function

Of course, much variation exists around this 'regional average' depending on age, density, etc. A tighter estimate can be derived by looking at conditions in stands of a particular density *and* age. Figure 4.16 displays several other 'predicted' cumulative distributions based on Installation 914[3] via Model 3.6, which is dissected into four

[2]Model 3.6 was used to produce this figure

[3]Installation 914 was used given it represented a stand of average SI_{30} (86.6), it has been measured

sections. These sections display how the distributions of predicted $DLLBH$ values change based on their age and original planting density. In order to obtain predicted $DLLBH$ values, the DBH and RD were extracted from Installation 914 based on TPA_0 at ages 12 and 20. With these three variables, $DLLBH$ was estimated and the predicted cumulative distributions were plotted.

The distributions of predicted $DLLBH$ values do hold with what one would expect given the two ages and planting densities. For example, as the installation progresses from age 12 (a) at 214 TPA_0 (9.6 RD ft.^{2}in.$^{-.5}$) to age 20 (b) (now at 27.7 RD ft.^{2}in.$^{-.5}$) there is a lower probability of observing branches less than 1 inch in diameter due to the lack of mortality. Conversely, as the installation progresses from age 12 (c) at 750 TPA_0 (23.96 RD ft.^{2}in.$^{-.5}$) to age 20 (d) (now at 52.66 RD ft.^{2}in.$^{-.5}$) the probability of observing a branch less than .7 inches increases signifying mortality due to competition.

The predicted cumulative distribution generated using Model 3.6 can now be compared to the empirical distribution for installation 914. As would be expected, Figure 4.17 displays more outliers, especially in larger branches. At 12 years and 214 TPA_0, roughly 60% of branches are below 1 inch in diameter and at 20 years this drops to roughly 50%. Compare this to Figure 4.16, where the change is roughly 75% to 50% at 214 TPA_0, respectively. At 12 years and 750 TPA_0, roughly 45% of branches are below 1 inch, while this jumps to nearly 80% by age 20. This same pattern occurs in Figure 4.16; however, the model projects more branches smaller than 1 inch, especially by age 20, even though the distributions shift in the same manner.

---

at 'early' and 'late' stages (12, 20 years), and had the most measurements (750) with respect to the first two criteria

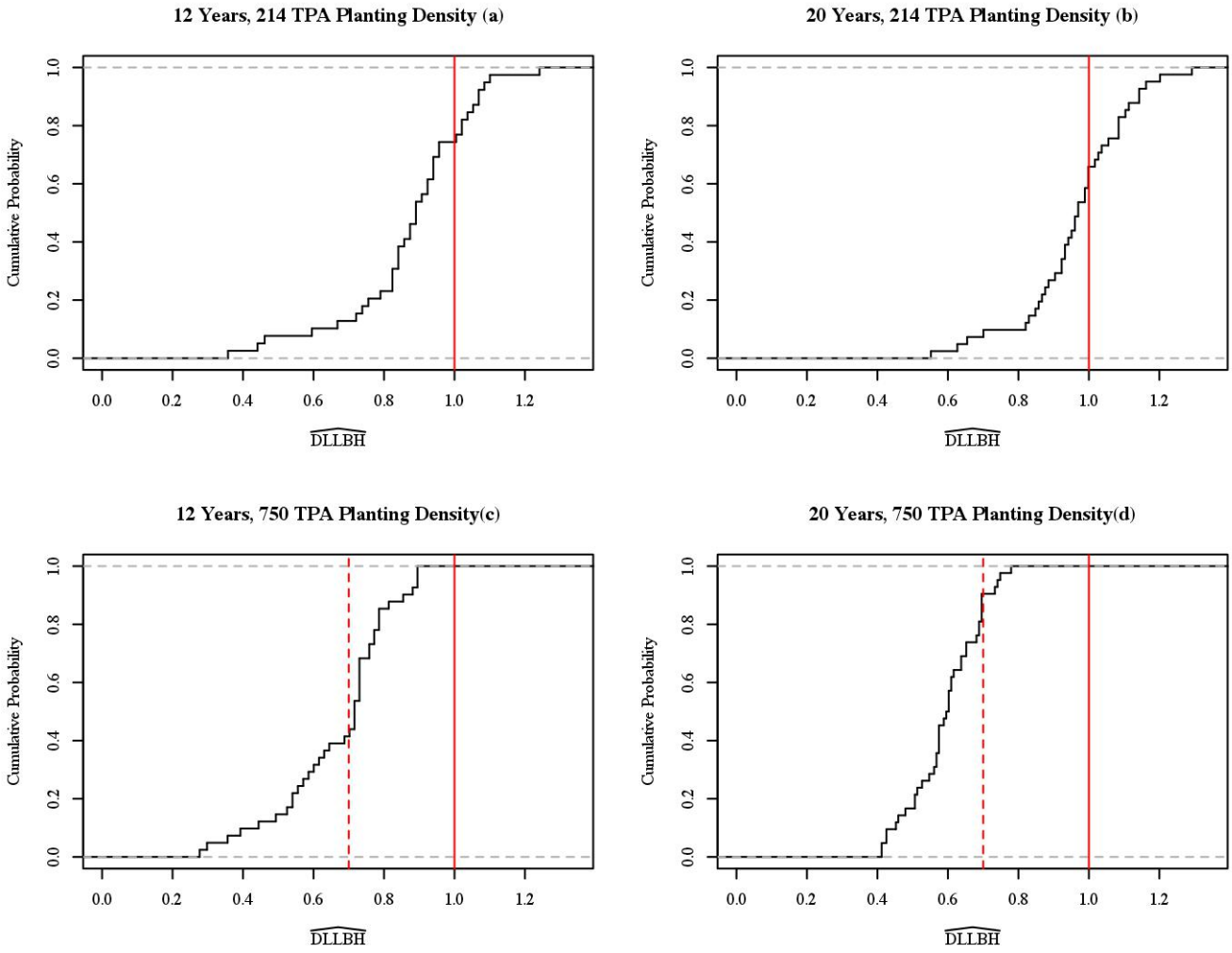

Figure 4.16: Predicted Cumulative Distribution Functions for Installation 914

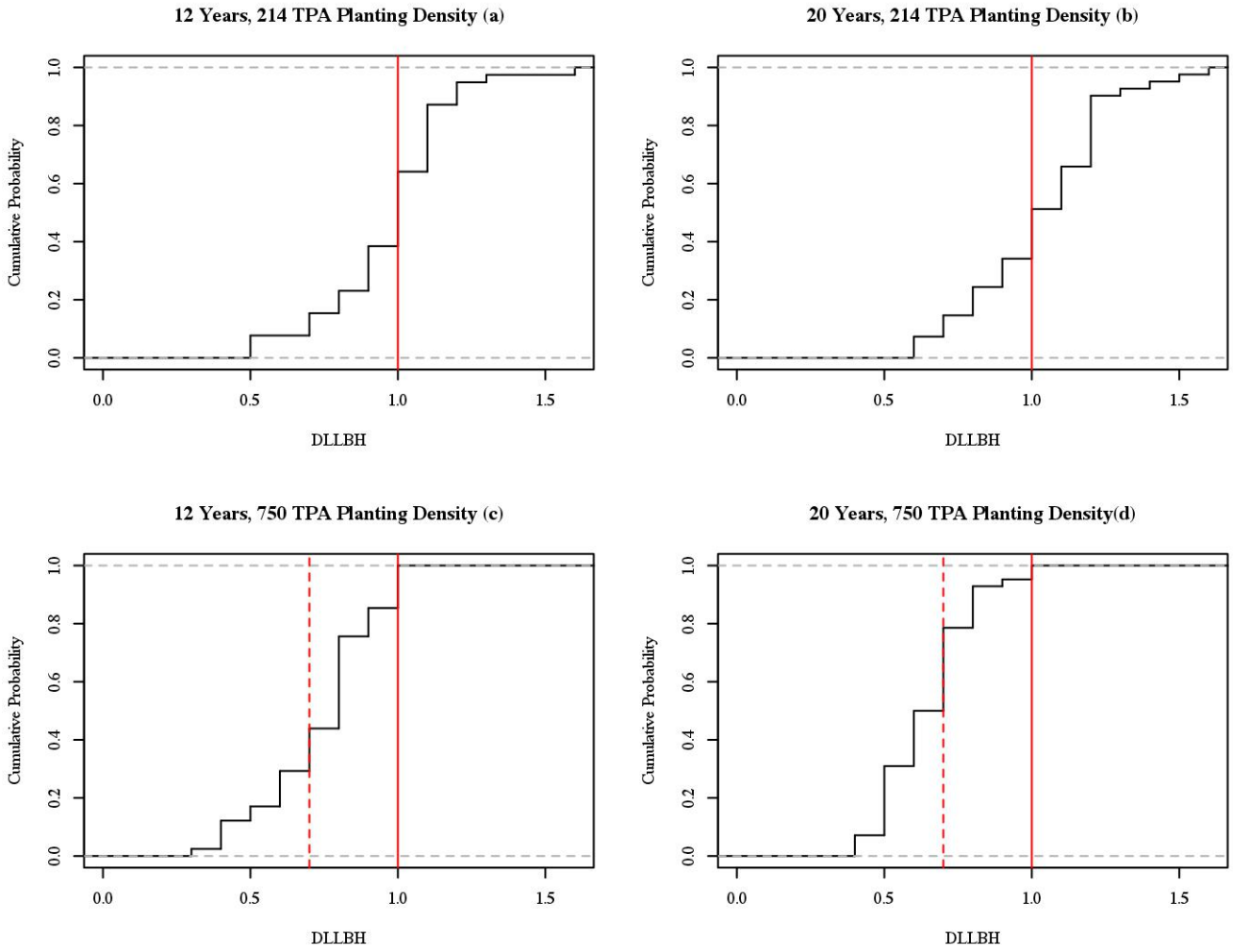

Figure 4.17: Empirical Cumulative Distribution Functions for Installation 914

Predicted and empirical distributions may be used to assess whether or not the product is meeting standards of the supplier or the purchaser. Clearly, if branches have been measured the empirical distribution suffices; however, the model may be used in contexts where branch sizes were not measured. Furthermore, both may be used as tools to assess whether or not changes in the manufacturing process (e.g. pruning or thinning) should be implemented.

4.5 Future Research

While this study has achieved the objectives presented in the Introduction, there are still several areas in which future research is necessary. First, the models should be validated on another dataset. While the projections were logical in this context, it is important to judge the ability of the model to perform based on data not used in model construction. In doing so, it would be best to use young stands of coastal Douglas-fir. Should there exists branch measurements on this stand, the model could be validated or nullified.

Second, the use of related rates in conjunction with the final model form would provide greater insight into branch growth, specifically relating $DLLBH$ growth to DBH growth. This process would involve simple partial differentiation of $DLLBH$ and DBH with respect to AGE. Armed with this knowledge, a temporal estimate of branch mortality might be constructed.

Chapter 5

CONCLUSION

This study examined two modeling methodologies to predict $DLLBH$ using a combined power exponential function. The first method examined admitting predictor variables as additional factors in the power function portion and linear terms in the exponential portion. The second method used DBH as the base and estimated the parameters with simple linear functions of tree, stand, and age variables.

While the intuitive approach would be to include all three types of covariates from the beginning, the idea was to start with tree-level given the allometric relationship between $DLLBH$ and DBH and build the model up. After tree-level based covariates were added, stand-level variables were introduced to the model. While these variables did not 'hurt' the modeling effort, their effects were not necessarily substantial. The use of BA_S proved to be the best stand-level metric for Model Type I, while RD was the driving variable in predicting the parameters on DBH for Model Type II. The outcomes of the models based on tree-level variables were perhaps more interesting. BR, which is essentially an interaction of CBH and HT, replaced CBH and HT for predicting parameters; however, it did not suffice in Model Type I on its own.

AGE was the final variable added to the model Types I and II because unlike most studies, this study could utilize repeated tree measurements. Again, the branches are not technically repeated given there is no guarantee that the same branches were measured from year to year; however, the same trees were measured and the $DLLBH$ was always recorded. The two models which included age were the best in each of their respective categories. When comparing both model forms, model Type II (3.6) was simpler and simultaneously provided better fit statistics. Furthermore, Model 3.6

preserved the variable allometric relationship between $DLLBH$ and DBH. For these reasons, Model 3.6 was deemed the superior model.

The final component of the study was to utilize Model 3.6 in a quality control context. A single installation was selected based on its average representation of growth, and $DLLBH$ projections were made in order to generate both predicted and empirical cumulative distributions. From these distributions, the purchaser or supplier of lumber can obtain an idea of how well the stand is conforming to specified needs based on properties such as lumber quality. As predicted by the model, the lower density stands display a higher probability of observing a value greater than a 1 inch threshold due to the lack of competition induced mortality. Conversely, the model predicted values that gave a higher probability of observing values less than a .7 inch threshold for dense stands, which is indicative of branch shrinkage due to mortality. Though the patterns in both the predicted and empirical cumulative distributions were similar as the stand progressed, the model is clearly unable to capture the natural amount of outliers in terms of larger branches. As a result, future research is necessary in order to obtain a better understanding of the distributions of predicted values, which most likely entails adjustment for the hierarchical structure of the data.

BIBLIOGRAPHY

[1] Baldwin, V.C., Peterson, K.D., Clark, A., Ferguson, R.B., Strub, M.R., and Bowever, D.R. 2000. The effects of spacing and thinning on stand and tree characteristics of 38-year-old loblolly pine. For. Ecol. Manage. **137**: 91-102. dpi:10.1016/S0378-1127(99)003040-0.

[2] Ballard, L A., and Long, J.N. 1988. Influence of stand density on log quality of lodgepole pine. Can. J. For. Res. 18: 911-916.

[3] Bates, D. M., Watts, D. G. Nonlinear Regression Analysis & It's Applications. USA. John Wiley & Sons, Inc. 1988.

[4] Benjamin JG, Kershaw JA, Weiskettel AR, Chui YH, Zhang SY. 2009. External knot size and frequency in black spruce trees from an initial spacing trial in Thunder Bay, Ontario. For. Chron. 85(4): 618-624 .

[5] Briggs, D. G. 2005. Assessing and Managing Stands to Meet Quality Objectives. In Harrington Constance A., Schoenholz, Stephen H. eds.; Productivity of Western Forests: A Forest Products Focus Gen. Tech. Rep. PNWGTR-642; U. S. Department of Agriculture, Forest Service Pacific Northwest Research Station, Portland OR. pp 141-152.

[6] Briggs, D., Ingaramo, L., and Turnblom, E. 2007. Number and diameter of breast-height region branches in a Douglas-fir spacing trial and linkage to log quality. Forest Prod. J. 57(9): 28-34.

[7] Briggs, D. G., Kantavivhai, R., and Turnblom, E. C. 2008. Effect of precommercial thinning followed by a fertilization regime on branch diameter in coastal United States Douglas-fir plantations. Can. J. For. Res. 38: 1564-1575.

[8] Briggs, D. G., Kantavivhai, R., and Turnblom, E. C. 2010. Predicting the diameter of the largest breast-height region branch of Douglas-fir trees in thinned and fertilized plantations. Forest Prod. J. 60(4):322-330.

[9] Briggs, D. G., E. C. Turnblom, and B. B. Bare. 2005. Non-destructive methods and process capability analysis to assess conformance of Douglas-fir stands to customer quality specifications. N. Z. J. Forestry Sci. 35(2/3):170-188.

[10] Fahey, T.D., J.M. Cahill, T.A. Snellgrove, and L.S. Heath. 1991. Lumber and veneer recovery from intensively managed young growth Douglas fir. USDA For. Serv. Res. Pap. PNW-RP-437. Portland, Oregon. 25 pp.

[11] Garber, D.M., Maguire, D.A., 2005. Vertical trends in maximum branch diameter in two mixed-species spacing trials in the central Oregon Cascades. Can. J. For. Res. 35: 295-307

[12] Hein, S., Weiskittel, A. R., and Kohnle, U. 2008. Branch characteristics of widely spaces Douglas-fir in south-western Germany: Comparisons of modelling approaches and geographic regions. For. Ecol. Manage. 256: 1064-1079.

[13] Maguire, D. A., Johnston, S. R., and Cahill, J. 1999. Predicting branch diameters on second-growth Douglas-fir from tree-level descriptors. Can. J. For. Res. 29: 1829-1840.

[14] Maguire, D. A., Kershaw, J. A. Jr., and Hann, D. W. 1991. Predicting the effects of silvicultural regime on branch size and crown wood core in Douglas-fir. For. Sci, Vol. 37, No. 5, November 1991.

[15] Maguire, D. A., Moeur, M., and Bennett, W. S. 1990. Simulating branch diameter and branch distribution in young Douglas-fir. *NEVER PUBLISHED?*

[16] Mäkinen, H., 1999a. Effects of stand density on radial growth of branches of Scots pine in southern and central Finland. Can. J. For. Res. 29, 1216-1224.

[17] Mäkinen, H., 1999b. Growth, suppression, death, and self-pruning of branches of Scots pine in southern and central Finland. Can. J. For. Res. 29, 585-594.

[18] Meredieu, C., Colin, F., and Hervé, J.-C. 1998. Modelling branchiness of Corsican pine (Pinus nigra Arnold ssp. laricio (Poiret) Maire) with mixed-effect models. Ann. Sci. For. **55**: 359-374.

[19] Protz, C.G., Silins, U., and Lieffers, V.J. 2000. Reduction in branch sapwood hydraulic permeability as a factor limiting survival of lower branches in lodgepole pine. Can. J. For. Res. **30:**: 1088-1095. doi:10.1139/cjfr-30-7-1088.

[20] Roeh, R.L., Maguire, D.A., 1997. Crown profile models based on branch attributes in coastal Douglas-fir. Forest Ecology and Management 96, 77100.

[21] Silviculture TAC (1991). *Stand Management Cooperative Field Procedures Manual: Douglas-fir version.* Stand Management Cooperative, University of Washington, Seattle, Washington.

[22] Sit, V., and Poulin-Costello, M. 1994. Catalog of curves for curve-fitting. Biometrics Information Handbook Series No. 4. British Colombia Ministry of Forests, Victoria, B.C.

[23] Uusvaara, O. 1989. Effect of spacing and site quality on branchiness and wood quality in Scots pine plantations, pp. 243253. In: James, R.N. and Tralton, G.L. (Eds) New Approaches to Spacing and Thinning in Plantation Forestry, Proceedings of an IUFRO Symposium 1014 Apr., Rotorua, New Zealand. Forest Research Institute, New Zealand. FRI Bull. 151.

[24] Vestøl, G.I., F. Colin, and M. Loubère. 1999. Influence and progeny and initial stand density on the relationship between diameter at breast height and knot diameter of Pcea abies. Scand. J. Forest Res. 14:470-480.

[25] Weiskittel, A.R., Hofmeyer, P.V., Seymour, R.S., and Kershaw, J.A. 2010. Modelling primary branch frequency and size for five conifer species in Maine, USA . Forest Ecology and Management 259: 1912-1921.

[26] Weiskittel, A.R., Maguire, D.A., 2006. Branch surface area and its vertical distribution in coastal Douglas-fir. Trees 20, 657-667.

[27] Weiskittel, A. R., Maguire, and D. A., Monserud, R. A. 2007. Response of branch growth and mortality to silvicultural treatments in coastal Douglas-fir plantations: Implications for predicting tree growth. For. Ecol. Manage. 251: 182-194.

[28] Woollons, R.C., Haywood, A., McNickle, D.C., 2002. Modeling internode length and branch characteristics for Pinus radiata in New Zealand. For. Ecol. Manag. 160, 243261.

Appendix A

ADDITIONAL TABLES

Table A.1: Description of 22 Installations

Installation	Year Planted	Age(s)* Measured	SI_{30}	Latitude	Longitude	Sample Size**
901	1985	14, 18, 22	98.6	46.7	123.2	728
903	1986	16, 20, 24	77.1	43.7	122.84	741
905	1987	12, 16, 20	89.9	43.3	124.0	710
910	1987	13, 15, 19, 23	80.6	47.0195	122.2	942
914	1989	12, 16, 20	86.6	44.6	123.3	750
915	1989	11, 15, 19	94.4	47.0	122.2	718
916	1989	13, 17, 21	81.5	44.9	123.3	868
917	1990	16	92.6	49.0	122.1	222
918	1990	10, 12, 16, 20	84.9	45.2	122.5	950
919	1990	11, 15, 19	90.9	47.2	123.9	758
922	1990	10, 14, 18	95.1	47.5	122.0	723
924	1990	10, 12, 16, 20	87.5	48.8	122.1	843
925	1990	11, 13, 15, 19	64.4	47.5	122.9	1009
926	1990	11, 13, 17, 21	91.7	46.2	123.2	966
929	1990	17, 21	69	NA	NA	58
932	1990	11, 15, 19	86.3	48.0	124.4	734
935	1990	10, 12, 16, 20	90.4	47.9	122.9	1029
937	1995	7, 9, 11, 15	100.1	44.4	122.7	948
938	1990	10, 12, 16, 20	79.7	45.2	122.5	946
942	1994	8, 12, 16	56.7	47.5	122.9	537
943	1994	7, 9, 11, 13, 17	83.7	46.7	123.2	1220
948	1993	14, 18	102.4	NA	NA	481

* Total Age

** Total $DLLBH$ measurements

Table A.2: Means and Standard Deviations by Target Densities

Variable.	100	200	300	440	680	1210
$DLLBH$	1.015 (.3799)	.8743 (.3072)	.8150 (.2587)	.7716 (.2522)	.6802 (.2257)	.6085 (.1976)
DBH	6.195 (3.315)	5.596 (2.884)	5.338 (2.525)	5.118 (2.392)	4.655 (2.068)	4.392 (1.928)
HT	31.69 (14.32)	31.40 (14.53)	32.15 (14.11)	32.18 (14.51)	32.11 (13.85)	33.24 914.29)
CBH	3.558 (4.349)	5.039 (6.185)	6.787 (7.637)	8.096 (8.465)	9542 (9.304)	12.12 (10.46)
HD	67.71 (19.45)	72.45 (17.89)	75.80 (16.63)	78.53 (16.95)	85.57 (18.50)	93.93 (22.95)
CL	28.13 (12.39)	26.37 (10.92)	25.37 (9.332)	24.09 (9.028)	22.57 (7.812)	21.11 (7.093)
CR	.8924 (.0837)	.8616 (.1076)	.8255 (.1330)	.7894 (.1485)	.7497 (.1688)	.6909 (.1868)
BR	.1076 (.0837)	.1384 (.1076)	.1745 (.1330)	.2106 (.1485)	.2503 (.1688)	.3091 (.1868)
BA_T	.2692 (.2490)	.2161 (.1949)	.1901 (.1619)	.1740 (.1468)	.1415 (.1155)	.1255 (.1028)
DBH_{REL}	.9867 (.2376)	.9886 (.2530)	.9866 (.2424)	.9924 (.2531)	.9988 (.2755)	1.010 (.3043)
BA_S	25.57 (22.14)	39.51 (32.41)	51.90 (38.28)	62.04 (43.42)	72.32 (46.83)	94.20 (51.32)
QMD	6.286 (3.073)	5.485 (2.646)	5.224 (2.247)	5.038 (2.108)	4.572 (1.744)	4.279 (1.512)
TPA	95.71 (15.80)	185.3 (39.58)	274.9 (44.22)	375.3 (93.78)	535.0 (132.3)	839.8 (197.7)
TPA_0	99.82 (13.25)	194.2 (38.72)	285.1 (45.17)	395.4 (97.31)	564.4 (136.1)	898.6 (197.1)
RD	8.987 (6.408)	14.81 (10.04)	20.33 (12.26)	25.10 (14.49)	31.09 (16.75)	42.67 (19.14)
SI_{30}	82.26 (9.559)	83.24 (11.77)	86.67 (11.82)	87.01 (11.33)	86.36 (9.705)	90.16 (12.08)

Table A.3: Summary of Model 1 (Tree-level)

Candidate Model	Variables Added	RSE	% Decrease	Comments
1	DBH	.2256		Illogical global behavior
1.1	1, HD	.1829	18.9	
1.11	1.1,CBH	.1744	4.6	$e^{(e*hd)}$ NS
1.111	1.11, HT	.1728	.92	STOP
1.112	1.11, CR	.1736	.46	STOP
1.12	1.1, HT	.1797	1.8	STOP
1.13	1.1, CR	.1749	4.4	
1.131	1.13,CBH	.1736	.74	STOP
1.132	1.13, HT	.1741	.46	STOP
1.14	1.1, BA	.173	5.4	
1.2	1, CBH	.1854	17.8	
1.21	1.2, HD	.1745	5.9	
1.211	1.21, HT	.1728	.97	STOP
1.212	1.21, CR	.1736	.56	STOP
1.22	1.2, HT	.1729	6.7	
1.221	1.22, HD	.1728	.0006	STOP
1.222	1.22, CR	.171	1.1	STOP (height$^{\beta}$ NS)
1.23	1.2, CR	.1844	.54	STOP
1.3	1, HT	.1799	20.3	Illogical global behavior
1.31	1.3, HD	.1797	.11	STOP
1.32	1.3, CBH	.1729	3.9	Illogical global behavior
1.321	1.32, HD	.1728		STOP
1.322	1.32, CR	.171	1.1	STOP (height$^{\beta}$ NS)
1.33	1.3, CR	.1741	3.2	Illogical global behavior
1.331	1.33, HD	.1741	0	Illogical global behavior($e^{\lambda HD}$ NS)

Table A.4: Summary of Model 1 (Tree-level) *continued*

Candidate Model	Variables Added	RSE	% Decrease	Comments
1.332	1.33, CBH	.171	1.8	STOP
1.34	1.3, BA	.1719	4.6	Illogical global behavior
1.341	1.34, CR	.1701	1	STOP
1.342	1.34, HD	—-	—	$e^{\lambda HD}$ NS
1.4	1, CR	.19	15.8	
1.41	1.4, HD	.1749	7.9	e^{λ} NS
1.411	1.41, HT	.1741	.46	STOP
1.412	1.41, CBH	.1736	.74	
1.42	1.4, CBH	.1844	2.9	
1.421	1.42, HD	.1736	5.8	
1.422	1.42, HT	.171	7.3	
1.43	1.4, HT	.1741	8.3	
1.431	1.43, HD	.1741	0	STOP
1.432	1.43, CBH	.171	1.8	(height^f NS)

Table A.5: Model Forms (Tree-, Stand - level)

Candidate Model	Variables Added	RSE	% Decrease	Comments
2	DBH, TPA_0	.1999	11.6	Logical global behavior
2.1	2, HT	.1759	12.2	$e^{\lambda_i^* TPA_0}$ NS
2.11	2.1, CBH	.1712	2.7	Illogical global behavior
2.2	2, QMD	.1889	5.5	
2.21	2.1, HT	.1732	1.5	STOP $e^{\lambda_i TPA_0}$, $e^{\lambda_i QMD}$ NS
2.22	2.1, RD	.1795	Increase	STOP qmd^{β_i}, rd^{β_i} NS
2.23	2.1, BA	.1801	Increase	STOP
2.3	2, SI30	.1977	1.1	STOP, Intercept NS
2.4	2, HD	.1782	10.9	Logical global behavior
2.41	2.4, HT	.1758	1.3	Illogical global behavior
2.42	2.4, CBH	.1731	2.9	
2.43	2.4, BA	.1729	3	Illogical global behavior
2.5	2, BA	.1801	9.9	Illogical global behavior
2.51	2.5, HT	.1728	4	Illogical global behavior
2.51	2.5, CBH	.1752	2.7	Illogical global behavior
2.6	2, RD	.1799	10	Illogical global behavior
2.61	2.6, HT	.1715	4.7	Illogical global behavior
2.62	2.6, HD	.1727	4	$TPA_0^{\beta_i}$ NS
2.63	2.6, QMD	.1795	.22	STOP

Table A.6: Model Forms (Tree -, Stand-, Age-)

Candidate Model	Variables Added	RSE	% Decrease	Comments
3	DBH, Age	.186		Illogical global behavior
3.1	3, DBH, TPA_0, Age	.1657		
3.11	3.1, HD	.1617	2.4	
3.111	3.11, CBH	.1598	1.2	Age^{λ_i} NS
3.112	3.11, SI30	.1603	.86	Age^{λ_i} NS
3.113	3.11, HT	.161	.4	
3.114	3.11, CR	.1599	1.1	Age^{λ_i} NS
3.12	3.1, HT	.161	2.8	Illogical global behavior
3.121	3.12, CBH	.1589	1.3	Age^{λ_i} NS
3.122	3.12, SI30	.1601	.56	
3.123	3.12, CR	.1596	.87	
3.2	3, CBH	.1629	1.7	Illogical global behavior
3.3	3, SI30	.1629	1.7	Illogical global behavior
3.5	3, CR	.1634	1.4	
3.6	3, BA	.1624	1.49	
3.7	3, QMD	.1662	+ .3	

Table A.7: Parameter Prediction Summary (tree-variables)

Variable	α_i	β_i	λ_i
HT	α_{01},α_{11}	-	-
CBH	α_{02}	β_{02}	-
BR	α_{03},α_{13}	β_{03},β_{13}	λ_{03},λ_{13}
CR	α_{04},α_{14}	β_{14}	λ_{04},λ_{14}
HD	α_{05}	-	-
BA	α_{06}	β_{06}	-
REL BAL	α_{07}	β_{07}	
BAL	α_{08}	β_{18}	λ_{19}

Table A.8: Summary of Tree-level Parameter Prediction Models

Candidate Model	Variables Added	RSE	% Decrease	Comments
4 (1)	DBH	.2256		Illogical global behavior
4.1	4, HT	.1869	17.2	Illogical global behavior
4.12	4.1, BR	.1781	4.7	Illogical global behavior
4.13	4.1, CR	.1831	2	Illogical global behavior
4.14	4.1, BAL	.1888	+1	Increased RSE
4.2	4, CBH	.1969	12.7	
4.3	4, BR	.1913	15.2	Logical global behavior
4.4	4, CR	.1926	14.6	
4.5	4, BAL	.2275	+1	Increased RSE

Table A.9: BR Class Breakdown

i	BR Range	Sample Size
1	[0, .07]	3373
2	(.01, .12]	3371
3	(.12, .18]	3370
4	(.18, .4]	3378
5	(.4, 1]	3390

Table A.10: Parameter Prediction Summary (stand-variables)

Variable	α_i	β_i	λ_i
TPA_0	-	β_{07},β_{11}	-
QMD	α_{08}	-	-
RD	α_{09}	β_{09},β_{19}	λ_{09},λ_{19}
SI_{30}	-	-	-

Table A.11: Summary of Tree-, Stand-variable Parameter Prediction Models

Candidate Model	Variables Added	RSE	% Decrease	Comments
5 (1)	DBH	.2256		Illogical global behavior
5.1	5,TPA_0	.2002	11.3	
5.11	5.1, Height	.1804	11.3	Illogical global behavior
5.111	5.11, RD	.1773	11.4	Illogical global behavior
5.2	5, RD	.1823	19.2	Logical global behavior
5.21	5.2, HT	.1736	4.8	Illogical global behavior

Table A.12: RD Class Breakdown

i	RD Range	Sample Size
1	[0, 7.7]	3416
2	(7.6, 15]	3413
3	(15, 24.9]	3372
4	(24.9, 40.3]	3376
5	(40.3, 90]	3305

Table A.13: Summary of Tree-, Stand-, Ave-variable Parameter Prediction Models

Candidate Model	Variables Added	RSE	% Decrease	Comments
6 (1)	DBH	.2256		Illogical global behavior
6.1	6, Age	.1885	16.4	
6.11	6.1, TPA_0	.1672	11.3	Logical global behavior
6.12	6.1, RD	.1627	13.69	Illogical global behavior m
6.13	6.1, BR	.1749	7.2	Illogical global behavior

Table A.14: AGE Class Breakdown

i	Age Range	Sample Size
1	[7, 11]	3416
2	(11, 14]	3413
3	(14, 16]	3372
4	(16, 19]	3376
5	(19, 24]	3305